Table of Contents

Chapter 4: Snow Observations and MEPS Forecasts for Haukeliseter

In this chapter the results of the snow surface observations, and the regional mesoscale forecast model at Haukeliseter are presented. On the basis of the methodology described in Chapter 2 it should be evaluated if the regional mesoscale forecast model MEPS predicts the same synoptic patterns as observed at the measurement site. Also, snow water content forecasted by MEPS is being compared with the retrieved vertical SWC at Haukeliseter. Shift to introduction background discussion!

Attention should be paid to the fact, that this study is unique because it uses state of the art vertical measurement to compare to an ensemble prediction forecast system. The motivation to compare regional model forecasts with vertical snowfall measurements resulted from a study by Joos and Wernli [2012]. They did sensitivity studies on the microphysical scheme of COSMO (COnsortium for Small-scale MOdelling) and found that the storm development depends on the correct vertical placement of the precipitation inside a modeled storm. Vertical precipitation placement determines the vertical profile of latent heating, and hence the generation of potential vorticity which in return shows if a storm strengthens or weakens. Correct vertical precipitation observations can then help to correctly assess model vertical precipitation patterns.

This study will give a first insight into comparing model observed with forecasts snowfall, for one particular extreme event, the 2016 Christmas storm.

4.1 The Christmas Storm 2016

One of the main factors, that made the Christmas 2016 storm so interesting is the fact that fronts passed over Norway during the six-day period. Associated to the occlusion passages and warm fronts the MASC took images of frozen and liquid particles at Haukeliseter.

This section will investigate meteorological quantities at Haukeliseter during the Christmas storm 2016. A comparison between the surface observations at Haukeliseter and the ECMWF analysis of the dynamic tropopause and geopotential thickness maps show that frontal transitions occurred on three days during the 2016 Christmas storm, 23, 25, and 26 December 2016 (Section 3.6). The frontal passages show up in the measurements and MEPS ensemble forecasts (Figures 4.1.1 to 4.1.4 and **????**).

Figures 4.1.1 to 4.1.4 and **????** displays the observations and model forecast quantities for sea level pressure, 2 m air temperature, 10 m wind, and precipitation on 21 to 26 December 2016 for the

Haukeliseter measurement site.
During all days the MEPS forecasts seem to predict similar sea level pressure, 2 m air temperature, and 10 m wind direction as were observed. Overestimations are simulated for wind speed (Figures 4.1.1 to 4.1.4 and **????**d) and surface precipitation amount (Figures 4.1.1 to 4.1.4 and **??????**).

Figures 4.1.5 to 4.1.7 presents the correlation of sea level pressure, 2 m air temperature, 10 m wind, and surface precipitation amount between the observations and the 48 h MEPS ensemble forecast. The relation for Haukeliseter observations and the MEPS forecast members is indicated with the regression calculated for each day. The scatter plots in Figures 4.1.5 to 4.1.7 show a good correlation for sea level pressure and 2 m air temperature. Sea level pressure has the best correlation of all variables. The MEPS forecast show a disagreement with southerly observed winds in Figure 4.1.6c, between 21 and 23 December 2016. A good agreement is seen for wind direction in Figure 4.1.6d for 24 to 26 December 2016. Wind speed is overestimated throughout the event and will be further investigated in Section 4.2.5 (Figure 4.1.7a, b). Surface precipitation amount agrees better between 21 to 23 December 2016 (Figure 4.1.7c) than during 24 and 26 December 2016 (Figure 4.1.7d). Figure 4.1.7c suggests a better correlation below 20 mm, for 21 to 23 December 2016 than above. A detailed discussion about the precipitation overestimation at the surface is given in Section 4.2.3.
Sea level pressure and 2 m air temperature usually have a good correlation by nature. Pressure and temperature take positive and negative values and a histogram would show a normal distribution. On the other hand, wind speed and precipitation, can only have positive values. In addition, the distribution for wind and precipitation is usually skewed, since more small values are observed, predicted than high values. Furthermore, precipitation is spatially dependent. It does not rain all over Norway the same amount at the same time.
On 23 and 26 December 2016, pressure decreases and increases, as well as temperature increases, and wind changes are present. Since these changes show up in the surface observations it is assumed that frontal boundaries passed through Haukelieseter. As described in Section 3.6 the ECMWF dynamic tropopause analysis (Figure 3.6.4a) shows more ridging at the DT level on 23 December 2016, than on the previous days. Warm air is advected closer to Southern Norway (Figure 3.6.4a). The low-pressure system approaches in the course of the day south-east of Iceland and hence stronger west to south-west winds are associated with the cyclone (Figure 3.6.4c). The MEPS forecast, initialised on 23 December 2016 at 0 UTC in Figure 4.1.2a simulates the sea level pressure observations and shows the decrease in pressure to 990 hPa after 12 UTC due to the passage of the occluded front. After the transition of the occlusion the pressure stays constant. Since warmer air is more advected to the north and the DT in Figure 3.6.4a shows a warm low-pressure core, an increase in temperature, from −3 °C to 0 °C, is observed and predicted at the measurement site (Figure 4.1.2b). The 10 m wind observations show a change from west to south and 10 min wind of 8 m s^{-1}. The 25 December 2016 (Figure 4.1.3) shows an increase of temperature to +5 °C, between 15 UTC and 17 UTC leading to the assumption of a warm sector passage in Figure 4.1.3b. The overall weather situation, described in Section 3.6, showed that a warm front as well as cold front influenced Norway, on 25 December 2016. Since pressure and wind do not indicate a change

related to frontal development (Figure 4.1.3a, **??**), it is assumed that only the warm air section between the warm and cold front is shown in the surface measurements at Haukeliseter (Figure 4.1.3b). Include L, H in the surface pressure images

As the cyclone moves to the north-east, further into the Norwegian Sea, a wind change is apparent in the ECMWF analysis (Figure 3.6.4c). First westerly winds and later south-westerly winds are associated with the low-pressure system. The MEPS forecast and observations in Figure 4.1.2c and d indicate a wind change from west to south with a slight decrease in wind speed.

On 23 December 2016, the evolution of the occlusion is also observed by an increase in precipitation. Before 18 UTC the surface accumulation shows light precipitation (Figure 4.1.2e). During the passage of the occlusion, the observed surface accumulation increases which is associated to continuous, heavy precipitation shown in Figure 4.1.2e.

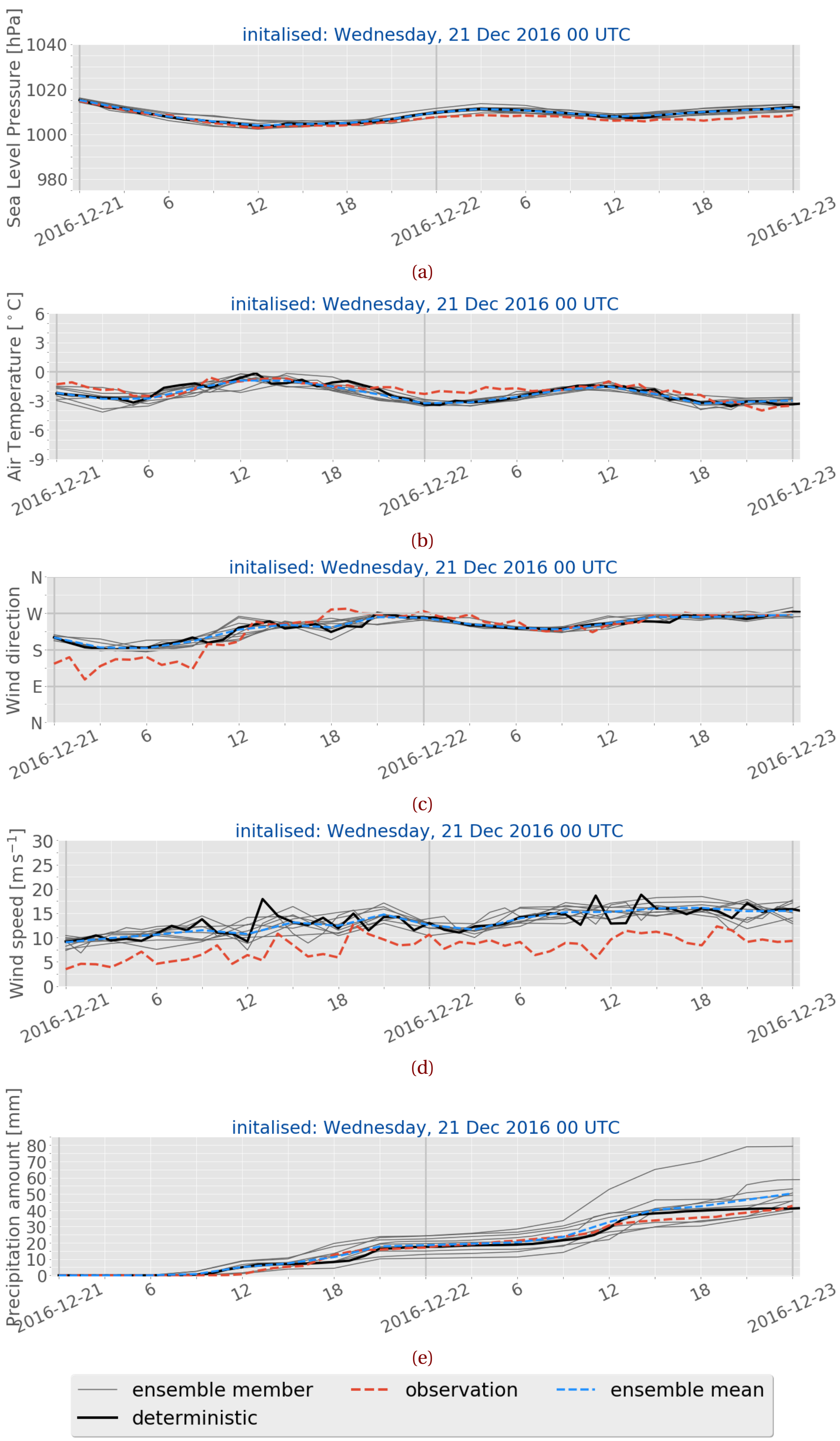

Figure 4.1.1: 48 h surface observations and MEPS ensemble forecasts initialised on 21 December 2016 at 0 UTC. Line representation according to the label. From top to bottom: sea level pressure, 2 m air temperature, 10 m wind direction and speed, and precipitation amount. *Continued on next page.*

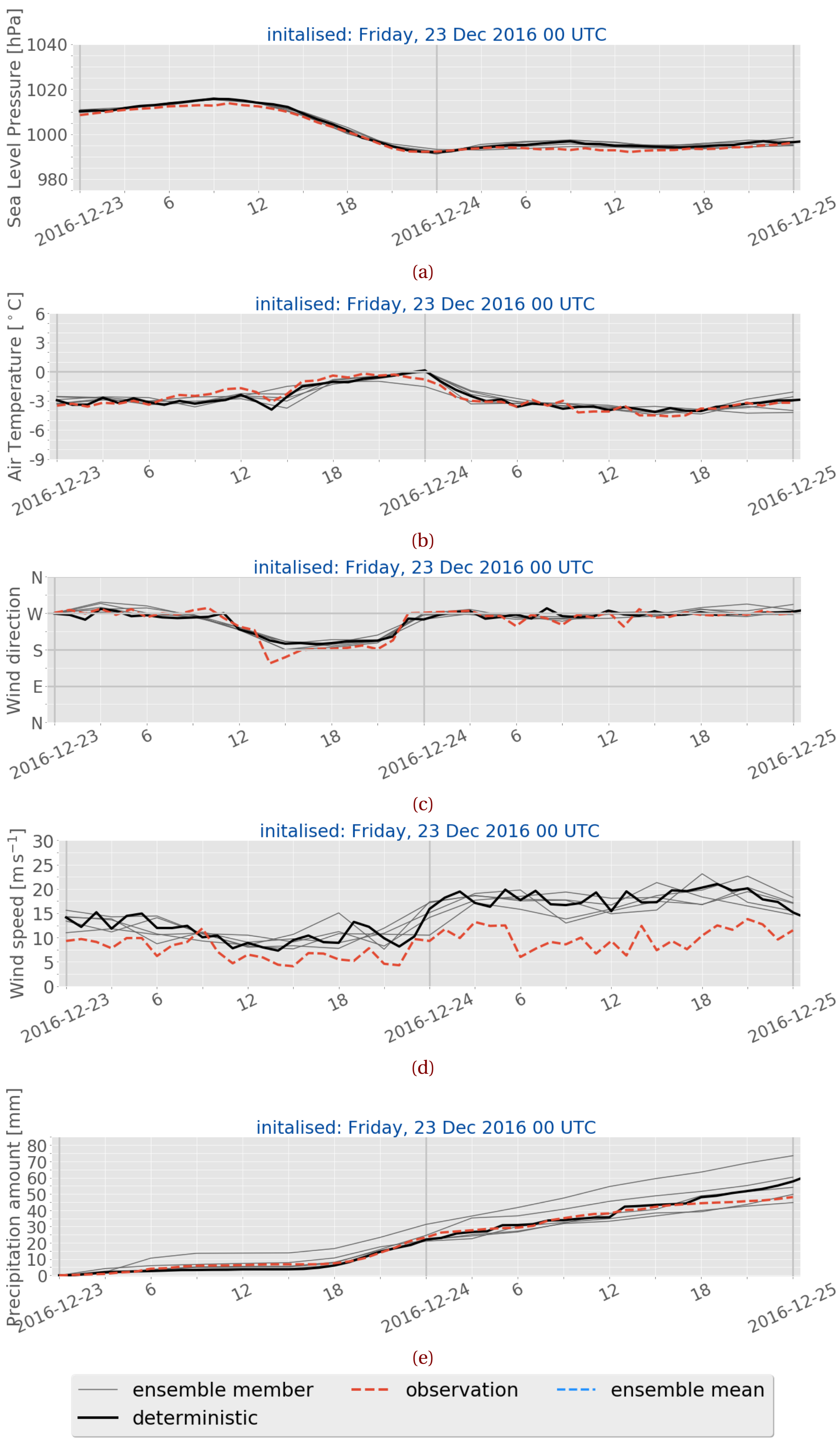

Figure 4.1.2: *(As Figure 4.1.1.)* Initialisation on 23 December 2016 at 0 UTC.

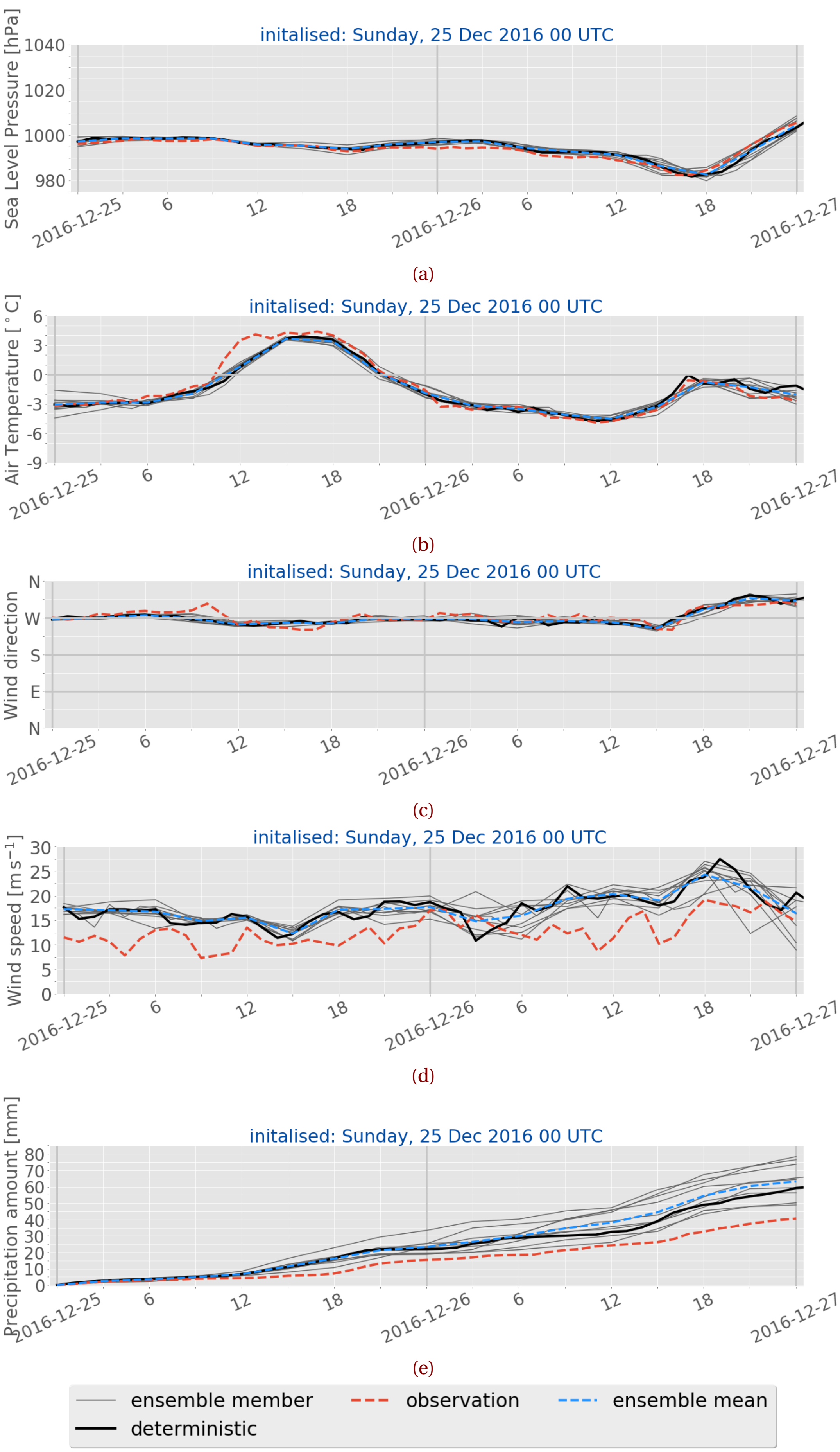

Figure 4.1.3: *(As Figure 4.1.1.)* Initialisation on 25 December 2016 at 0 UTC.

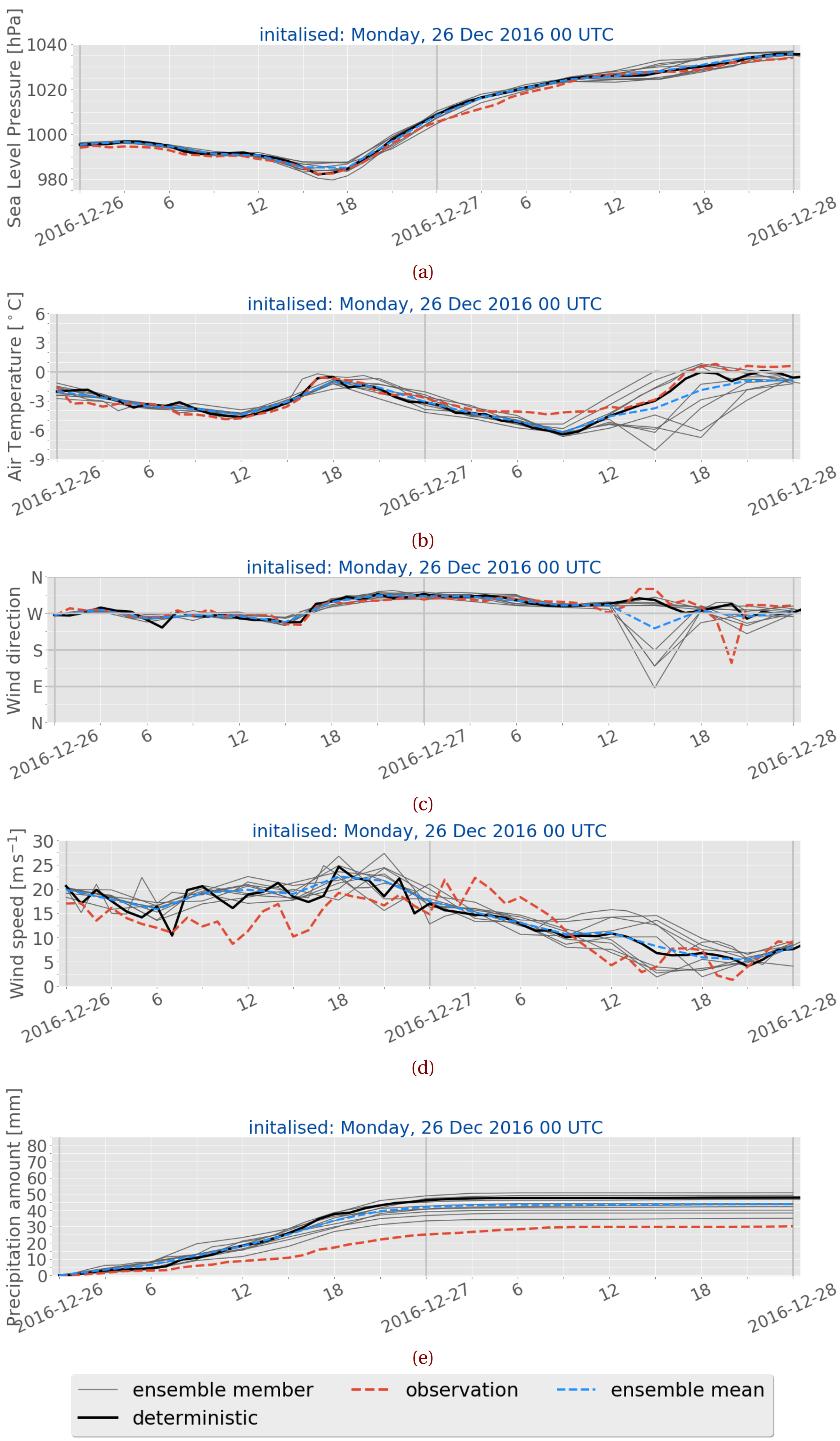

Figure 4.1.4: *(As Figure 4.1.1.)* Initialisation on 26 December 2016 at 0 UTC.

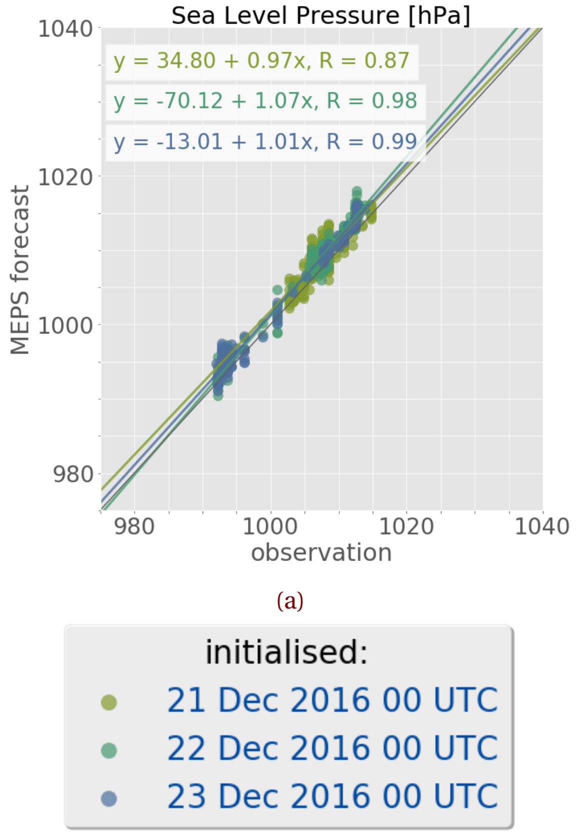

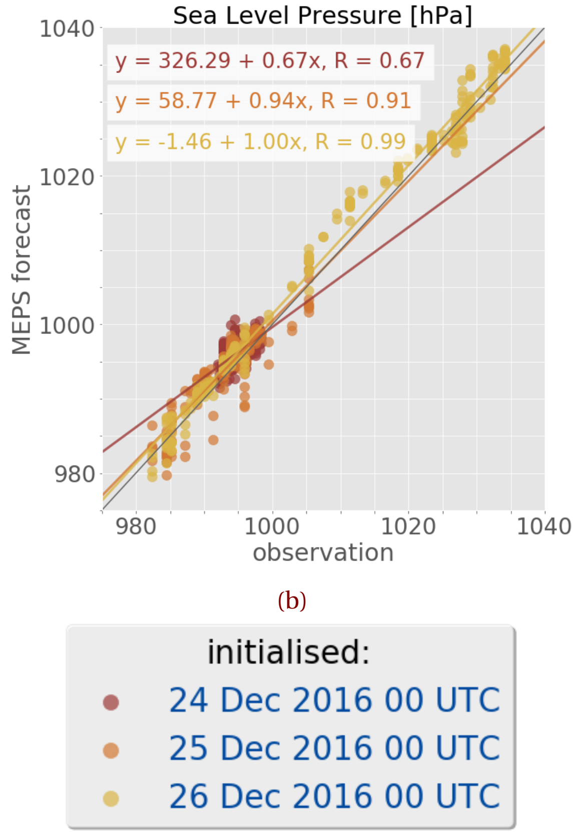

Figure 4.1.5: Scatter plots for sea level pressure observations and ensemble forecasts initialised for 21 to 23 December 2016 (a) and for 24 ton 26 December 2016 (b) The 48 h scatter values indicate each day, showing the 1 h and 3 h ten ensemble member forecasts respectively. The linear regression of all ensemble member for each individual day is presented together with the correlation coefficient *R*.

Similar patterns as on 23 December 2016 is seen for the evolution of the occluded front on 26 December 2016 in the ECMWF analysis Figure 3.6.7a and 3.6.7c. In this case the low-pressure system was located north of Møre and Romsdal in the Norwegian Sea. In the morning the cyclone is located east of Iceland and in the course of the day it moves closer to the coast of Norway (Figure 3.6.7b and 3.6.7d). Before landfall at 16 UTC, a pressure decrease occurs at Haukeliseter (Figure 4.1.4a). During the development of the occluded front, the pressure reaches its lowest point of 985 hPa (Figure 4.1.4a) and increases afterwards during the dissipation of the 2016 Christmas storm.

Since the cyclone was surrounded by colder air (south of the low-pressure system in Figure 3.6.7a), first a drop and then an increase of temperature were observed and forecasted by MEPS (Figure 4.1.4b). An indication of the occlusion evolution is also visible in the 10 m wind observations and MEPS predictions in Figure 4.1.4c and d. On 26 December 2016 at 0 UTC, the low pressure system is east of Iceland (not shown), moving closer into the Norwegian Sea by 12 UTC (Figure 3.6.7a and 3.6.7c). Surface westerly winds are associated to the cyclone in the Norwegian Sea, and impinging on the West coast of Norway Figure 3.6.7c. The wind measurement and MEPS forecast in Figure 4.1.4c and 4.1.4d, show a westerly gale of up to 18 m s^{-1} at Haukeliseter before 12 UTC. The centre of the occluded front is located over Norway at 18 UTC, and the pronounced

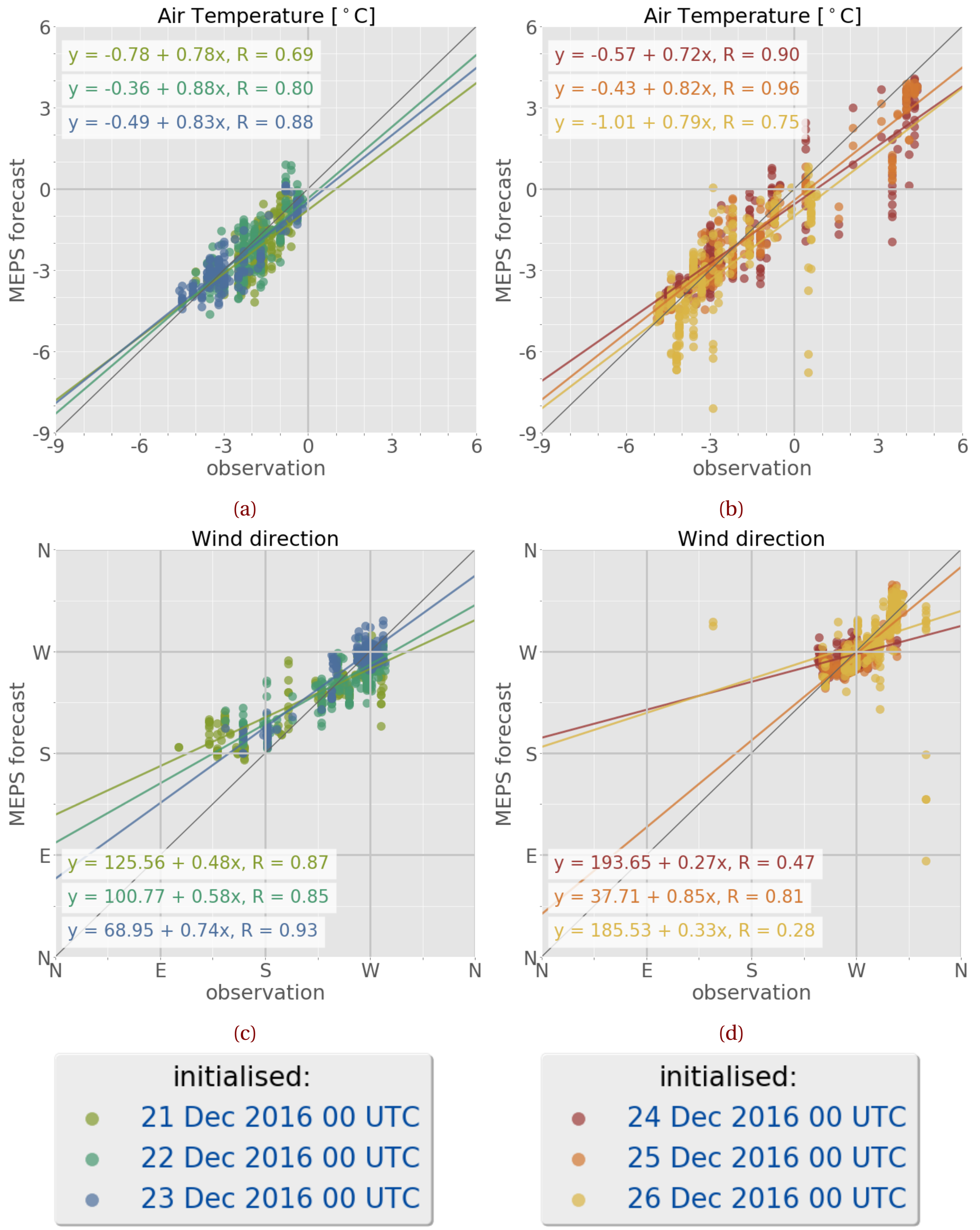

Figure 4.1.6: *(As Figure 4.1.5.)* From top to bottom: (a, b) 2 m air temperature, (c, d) 10 m wind direction.

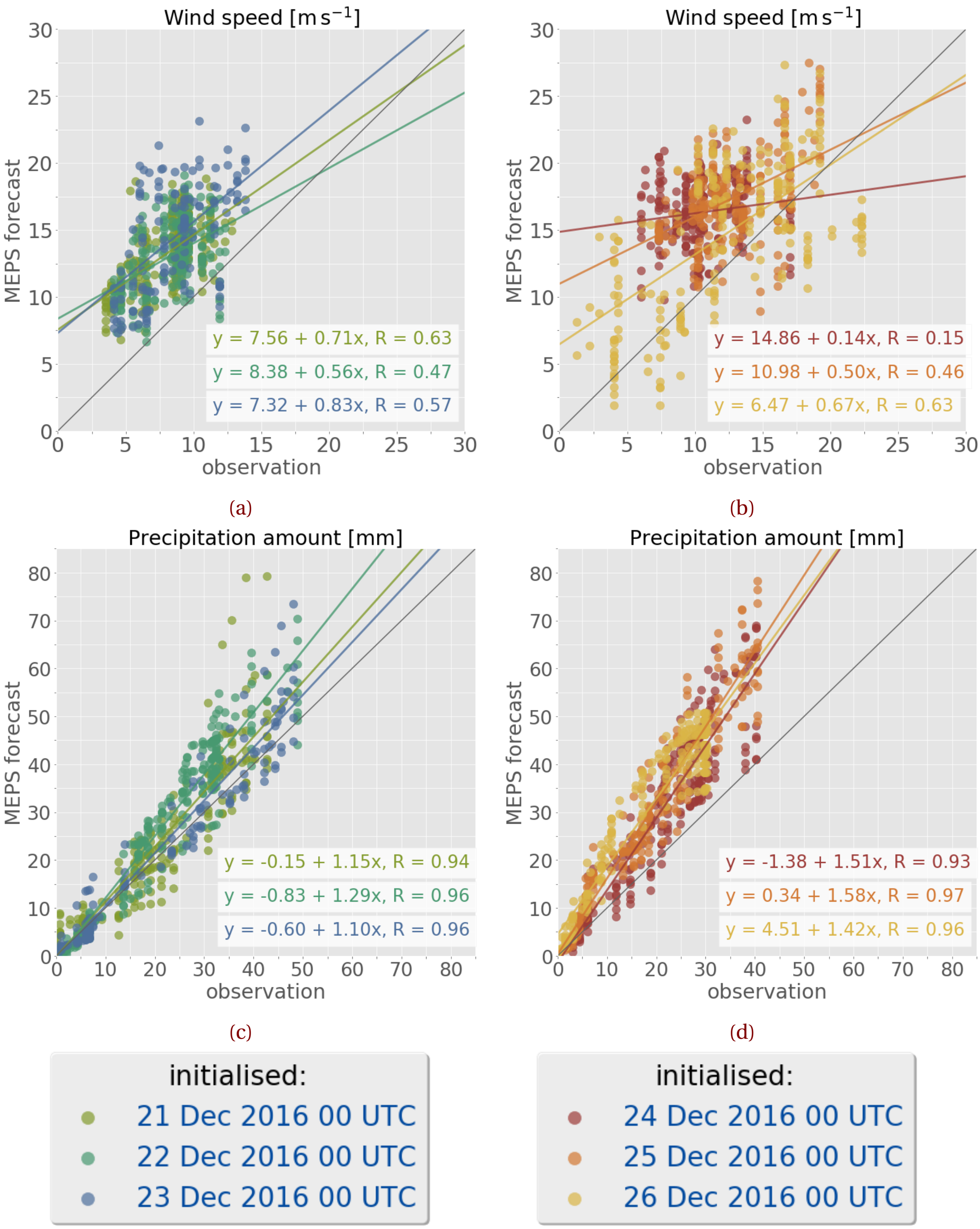

Figure 4.1.7: *(As Figure 4.1.5.)* From top to bottom: (a, b) 10 m wind speed, (c, d) surface precipitation amount comparing double fence observations to 48 h MEPS forecasts.

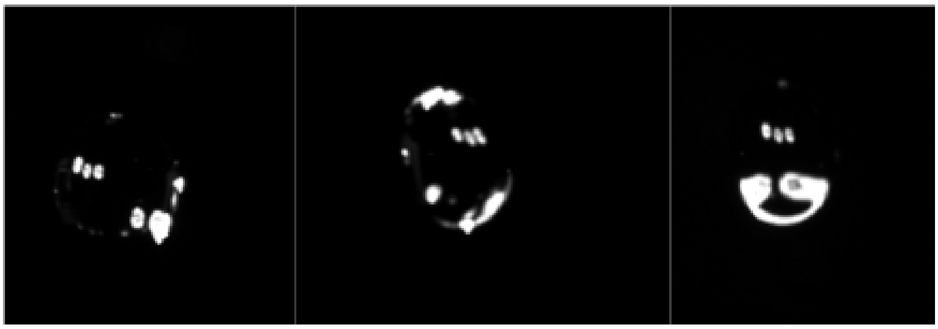

Figure 4.1.8: MASC images of falling water drops observed on 25 December 2016 at 17 UTC from three different angles. Not all parts of the liquid sphere are equally illuminated.

surface pressure gradient, in Figure 3.6.7d, indicate an increase in surface wind with a north-west wind direction. During this transition of the occlusion, the wind direction changes to north-west with higher observed wind speeds up to 20 $m\,s^{-1}$ (Figure 4.1.4c and 4.1.4d).
Precipitation is continuing throughout the day, with light to moderate precipitation before the occlusion passage seen in Figure 4.1.4e. Heavy precipitation related to the occlusion, around 16 UTC, is followed by moderate to light precipitation on 26 December 2016.

On 23 December 2016 a cyclone is south of Iceland (Figure 3.6.4) and precipitation was associated to the transition of the occlusion. While 26 December 2016 precipitation was associated with the landfall of an occlusion. 25 December 2016 was marked by the transition of a warm sector. The ECMWF analysis shows a pronounced upper level ridge at the dynamic tropopause (Figure 3.6.6a). The cyclone core is south east of Iceland in Figure 3.6.6a with two associated frontal boundaries. While the warm front is approaching the west coast, the cold front is north-west of Great Britain. In Figure 3.6.6c, the tail of the cold front moved into lower latitudes, following the slowdown of the front, leading to a stationary frontal boundary. Furthermore, the mid-latitude jet is aligned with the surface frontal boundaries (Figure 3.6.6a), while the Haukeliseter site is located below the the midlatitudal jet (Figure 3.6.6c).
Neither pressure nor wind observations and forecasts in Figure 4.1.3a, c, and d, indicate the evolution of any frontal boundary. The only indication of a transition could be seen in the increase and then decrease of temperature at 11 UTC until 21 UTC (Figure 4.1.3b). In Figure 4.1.3c, a small wind direction change from west to north-west is observed by the wind mast at 10 UTC. This is not forecasted by MEPS, as it rather estimated strong westerly winds.
Particle images taken by the MASC are available on 25 December 2016, during the transition of the warm sector in Figure 4.1.8. Without theses images taken around 17 UTC it would only be possible to verify that liquid precipitation occurred with the optical precipitation detectors at the Haukeliseter site. Together with the increase in surface temperature (Figure 4.1.3b) it can be concluded that the warm sector of the Christmas 2016 event passed by the measurement site.

The comparison between the ECMWF analysis (Section 3.6) and the observations at the measurement site (**??**), allow to conclude that the ensemble member forecast system MEPS covers the prediction of large scale phenomena like occlusions and fronts, as well as liquid precipitation at the surface.

The scatter plots for observations and MEPS forecast show good correlation for most variables (Figures 4.1.5 to 4.1.7). The best agreement for pressure is reached on 26 December 2016 (Figure 4.1.4a), when the Christmas storm hit land and dissipated after the evolution of the occlusion at 16 UTC. Dahlgren [2013] showed an improvement of sea level pressure forecast for AROME, by including large scale boundary conditions for ECMWF into the regional model. The observation-model comparison by Dahlgren [2013] showed a decrease of pressure bias with lead time after 24 h with the use of pressure mixing. Since surface pressure is in good agreement with the observations, it is assumed that the warm front did not pass through Haukeliseter on 25 December 2016 and only the warm sector associated with the 2016 Christmas storm is observed. This shows a quite detailed forecast ability of MEPS, as from the ECMWF analysis, in Figure 3.6.6a, it is not quite clear if the warm front could have passed through. To be sure that the warm front did not pass through Haukeliseter, or whether it is a predictive error of MEPS, surface pressure, temperature and wind should be compared to the nearest grid point of the global forecast model ECMWF to verify this result.

Figure 4.1.6b displays a moderate correlation between observation and the 48 h MEPS ensemble member forecast system. In general, MEPS underestimates the observed 2 m air temperature, but MEPS estimated the temperature changes at the correct occurrence for 23, 25, and 26 December 2016. This thesis uses only one extreme event during Christmas 2016 at Haukeliseter. Figure 4.1.9b shows warm and cold biases for 23 and 26 December 2016, respectively for Haukeliseter during the Christmas 2016 storm. On 25 December 2016, within the warm sector, a cold bias was observed, underestimating the temperature when compared to the observation. The forecasts for 23, 25, and 26 December 2016 show calculated mean absolute error values (Equation (2.7.5)) below 1 K in Figure 4.1.10b. In the verification report of Met-Norway MEPS deterministic forecast is verified against observations for December 2016 to February 2017 [Homleid and Tveter, 2016]. For December 2016 the 2 m air temperature had no bias within the Norwegian model domain. The Norwegian mean absolute error for 2 m air temperature was 1.6 K [Homleid and Tveter, 2016]. The mean absolute error for the Christmas 2016 storm is within the Norwegian December mean for the deterministic forecast. This does not necessarily show how well the forecast predicted the extreme event, since only one storm is studied at one site in Norway. The previous operational deterministic forecast model AROME-MetCoOp showed a cold bias of 2 m temperature for the Norwegian mean, during winter 2013 with the introduction of AROME-Norway and later AROME-MetCoOp [Müller et al., 2017]. The mean error for the Norwegian model domain of AROME-MetCoOP estimated by Müller et al. [2017] is smaller than 1.8 K for the surface 2 m air temperature in December 2014.

During the Christmas storm 2016, high wind speeds were observed at the Haukeliseter site (Figure 4.1.2d, 4.1.3d and 4.1.4d). According to Müller et al. [2017] high wind speeds are significantly better simulated for AROME-MetCoOp compared to ECMWF's forecast for the model domain. MEPS predictions of wind speed in Figure 4.1.2d, 4.1.3d, and 4.1.4d still display an overestimation of wind speeds throughout the event. Furthermore, the correlation of observations and wind speed in Figure 4.1.7a and b show an overestimation for stronger wind speeds on 24 to 26 December 2016 than for 21 to 23 December 2016. The mean error for wind speed during the Christmas storm is ranging from 0 m s^{-1} to 7 m s^{-1} for 48 h lead time (Figure 4.1.9d). During the extreme storm, the highest mean absolute error of 10 m s^{-1} occurs for initialisations on 24 December 2016 (Figure 4.1.10d).

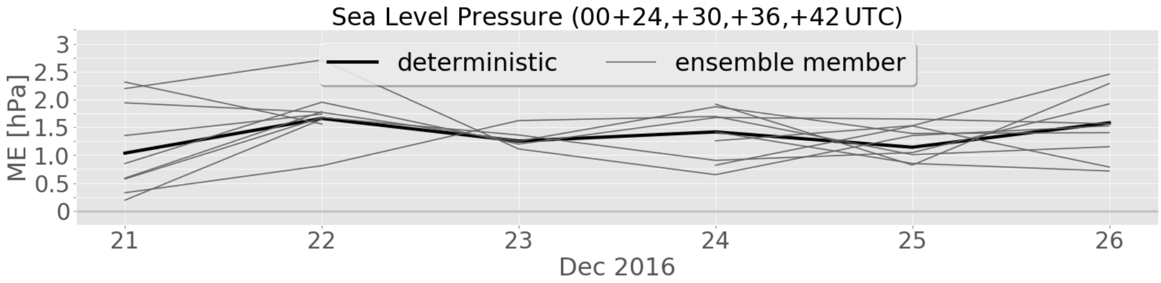

(a)

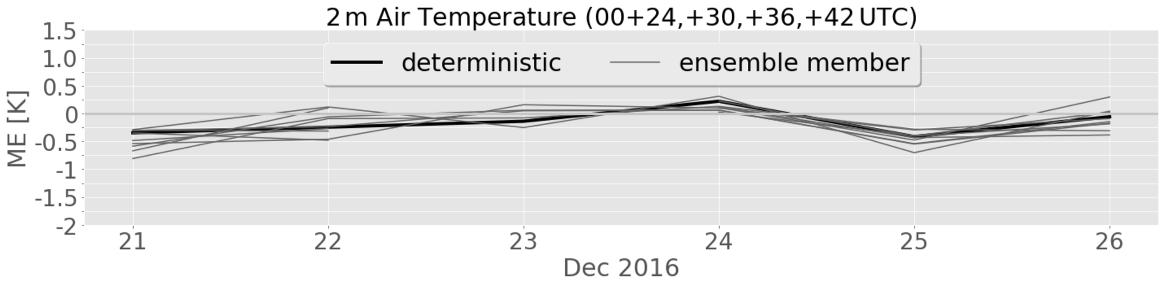

(b)

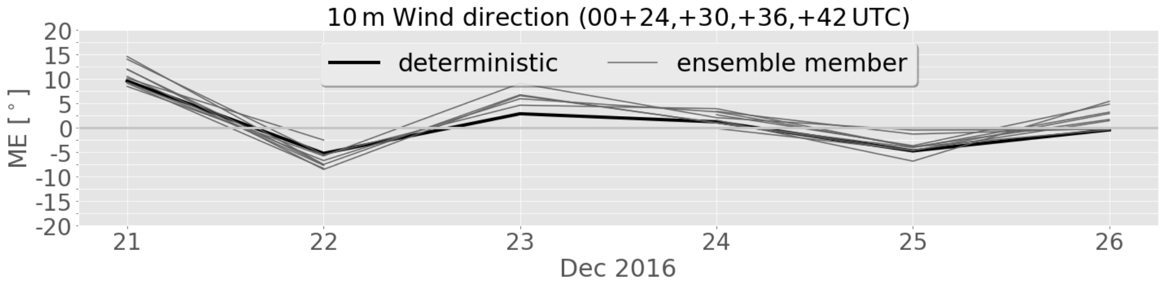

(c)

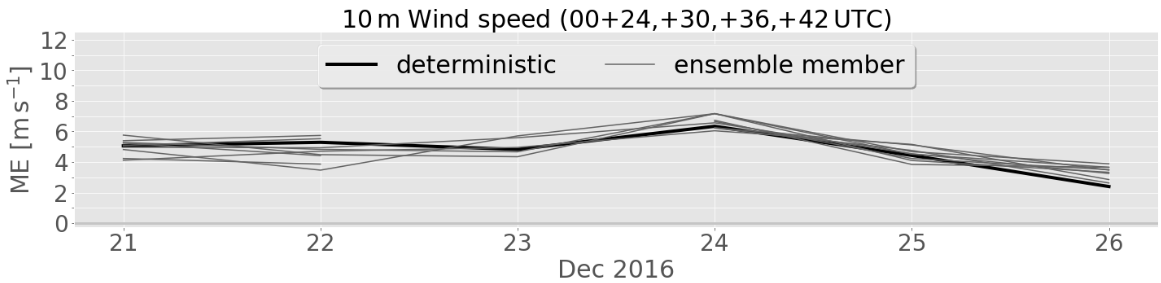

(d)

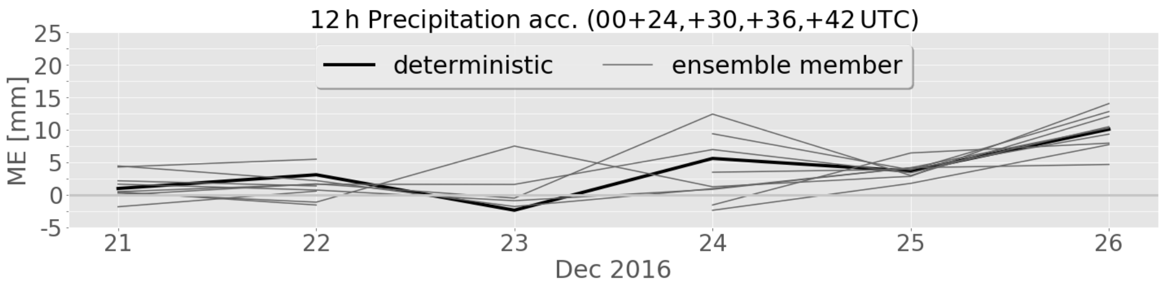

(e)

Figure 4.1.9: Mean error of surface variables for all ten ensemble members at Haukeliseter, initialisations at 0 UTC with lead times from 6 h to 24 h. From top to bottom, sea level pressure (a), 2 m air temperature (b), 10 m wind direction (c), 10 m wind speed (d), precipitation accumulation for 12 h surface accumulation (e).

The inaccuracy for wind speeds is an already known difficulty in the deterministic version of MEPS [Müller et al., 2017]. Müller et al. [2017] presented, that AROME-MetCoOp wind speed prediction generally agreed better with observations for wind speeds between 3 $m\,s^{-1}$ to 13 $m\,s^{-1}$ than ECMWF forecasts did, showing the advantage of a high-resolution weather model. Furthermore, with increasing wind speed the forecast accuracy for the Norwegian mean decreased with a mean absolute error below 2 $m\,s^{-1}$ for 6 h to 24 h lead times, in December 2014 in AROME-MetCoOp. Müller et al. [2017] case study showed a slight underestimation of ECMWF 10 m wind compared to the Norwegian AROME-MetCoOp forecast for February 2015. On 24 December 2016, the mean absolute error is more than fives times as high as the monthly averaged value for the Norwegian forecast domain (2 $m\,s^{-1}$ for 6 h to 24 h forecast time) from Müller et al. [2017]. In December 2016, the mean absolute error for the Norwegian mean of the deterministic forecast was 2 $m\,s^{-1}$ [Homleid and Tveter, 2016]. The difference between the mean absolute error during the event and the monthly averages of Met-Norway, is firstly related to the comparison of a long term study of Müller et al. [2017]. Secondly to a month average mean absolute for the Norwegian model domain [Homleid and Tveter, 2016, Müller et al., 2017], and third to the location of Haukeliester (orographic effect, Section 4.2.5).

Haukeliseter is a measurement site exposed to high wind speeds [Wolff et al., 2013, 2015]. The ensemble prediction system MEPS seems to still have issues forecasting the wind speed correctly in mountainous terrain. A detailed insight to the orographical wind influence will be discussed in Section 4.2.5.

Pressure, temperature, and wind changes for the occlusion transition on 26 December 2016 were already forecasted for initialisations on 25 December 2016 (Figure 4.1.3), only wind speed and precipitation seem not to agree with the observations at Haukeliseter. The same is true for 25 December 2016, when the warm sector passes through Haukeliseter.

Figures 4.1.1 to 4.1.4 and **????**e illustrate the surface precipitation amount observed and predicted by MEPS for Haukeliseter. MEPS overestimation is shown for precipitation when the cyclone intensifies and gets closer to Norway on 24, 25 and 26 December 2016. The surface observations and MEPS predictions in Figure 4.1.7c and d show an overestimate for 24, 25 and 26 December 2016, whereas on 21, 22, and 23 December 2016 the surface accumulation is balanced for predictions up to 30 mm. Any reasons for the overestimation of precipitation accumulation on the ground will be further analysed and discussed in Section 4.2.3. I HAVE TO SOMEHOW MERGE THIS IN, BUT HOW? What could be still a weakness that the model overestimates the wind speed? In Müller et al. [2017]: change from ECOCLIMAP1 because the surface roughness was too low and followed high wind speeds? Is this still the case for MEPS? High wind speeds followed also from wrongly adressed 'permanent snow'. Do not use 'orographi drag' in AROME-MetCoOp, could that lead to the too high estimated wind? When 'canopy drag' was changed saw increase in SBL drag which followed a decrease in wind speed. But AROME-MetCoOp is able to forecast high wind speeds, while ECMWF is not.

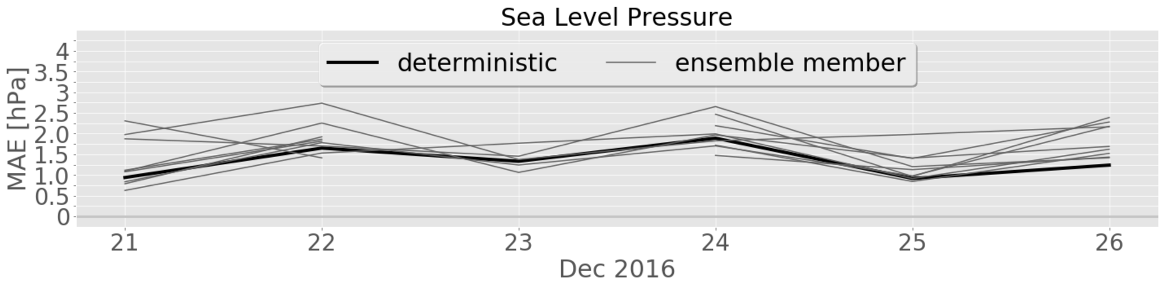

(a)

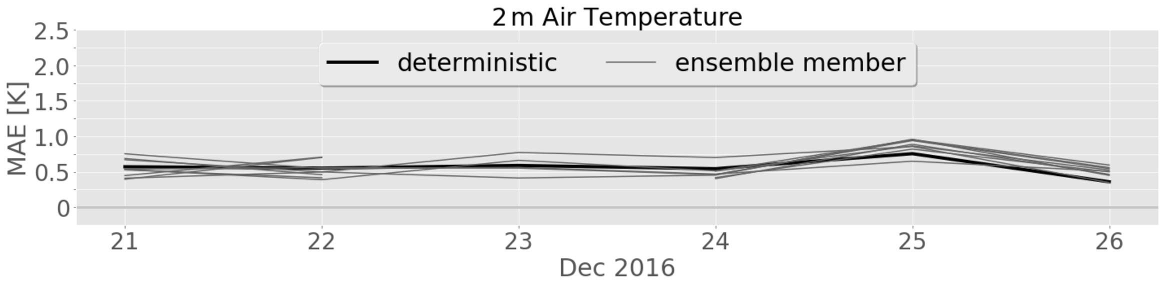

(b)

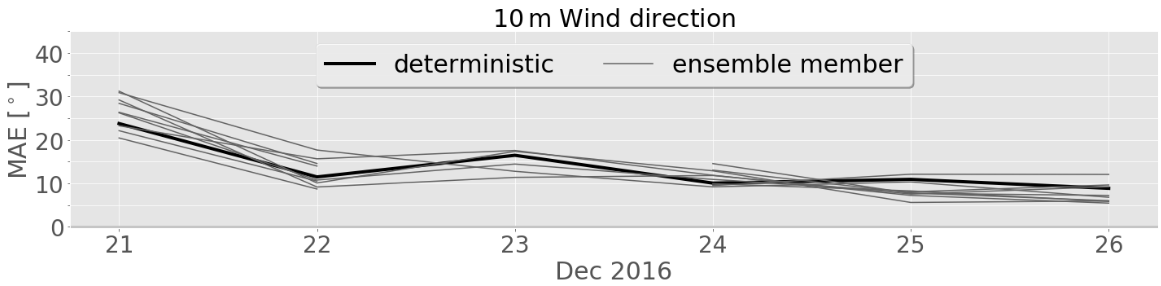

(c)

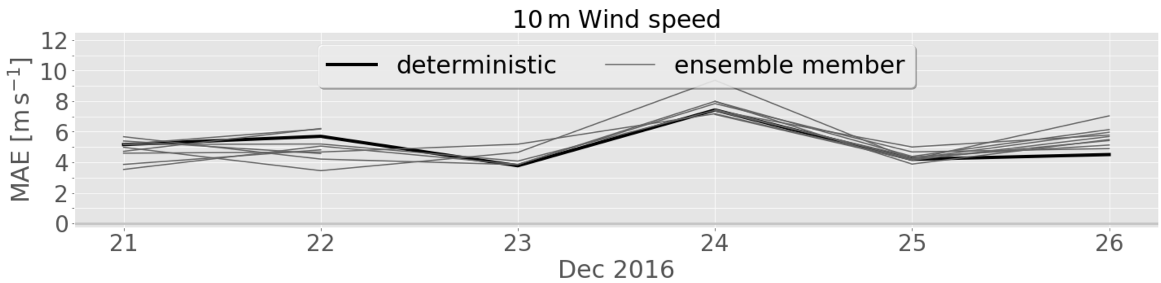

(d)

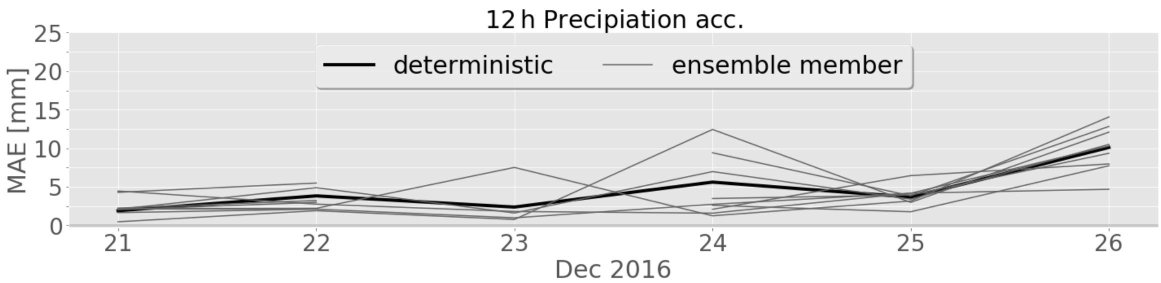

(e)

Figure 4.1.10: Mean absolute error (a, b, c, d, e) of surface variables for all ten ensemble members at Haukeliseter, initialisations at 0 UTC, valid for 48 h. From top to bottom, sea level pressure (a), 2 m air temperature (b), 10 m wind direction (c), 10 m wind speed (d), precipitation accumulation for 12 h surface accumulation (e).

Overall, for initialisations on 21 to 23 December 2016 (Figures 4.1.5 to 4.1.7) the forecast is best for all variables. The large-scale weather pattern seems to be more predictable as long as the weather situation is not extreme. The correlations for the forecasts between 24 and 26 December 2016 (Figures 4.1.5 to 4.1.7) suggest as MEPS may have difficulties predicting the intensification and associated pressure decrease of the Christmas 2016 storm at Haukeliseter. The prediction of pressure fits well on all days (Figure 4.1.5a, b) compared to temperature (Figure 4.1.6a, b), wind direction (Figure 4.1.6c, d), wind speed (Figure 4.1.7a, b), and precipitation (Figure 4.1.7c, d). The greatest difficulty MEPS has, is with the prediction of wind speed during the entire extreme event. The rainfall, however, fit well for 23 December 2016 (Figure 4.1.2e and 4.1.7c), but MEPS has problems predicting the accumulation of surface precipitation amount correctly for the extreme days of the 2016 Christmas storm, 24 to 26 December 2016 (Figure 4.1.3e, 4.1.4e, and 4.1.7d).

Figure 4.1.5 and 4.1.6 have shown good agreement of ensemble member forecasts to observations. It is not expected that ensemble members agree they should just give a variability around the observations, that is why ensemble member prediction exists (Section 2.5). Based on the uncertainty in observations the solution space that is possible has to be understood. The model is not adjusted to present the extreme event particularly well as it is adjusted to go towards the climate norm. Nevertheless should extreme events be within the spread of

4.2 Snowfall

After the analysis of meteorological quantities, the snowfall at Haukeliseter during the Christmas storm will be investigated.
First the results from the optimal estimation retrieval scheme will be examined and compared to the observations of the double fence. After the overestimation of surface accumulation will be analysed, followed by a vertical comparison of snowfall observations and predictions. The sections finishes with the relation between wind and precipitation related to the surrounding topography at Haukeliseter.

4.2.1 Sensitivity of the Optimal Estimation Retrieval

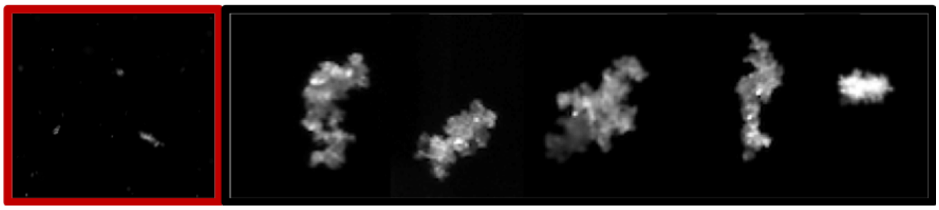

Figure 4.2.1: MASC observations during the Christmas storm 2016. Left (red frame), small ground-up blowing snow particles. Five images on the right, rimed particles.

Include some more specific: Which observations, which quantity was used to generate the optimal estimation retrieval? The optimal estimation retrieval scheme for snowfall was applied to the six-day Christmas 2016 storm event. MASC images of snowfall during the event were used to guide the selection of the appropriate particle model and PSD input for the retrieval scheme. In this section, the sensitivity of retrieval results to these inputs is explored for the 22 December 2016. This day is used as an example day because it showed the smallest difference between double fence gauge and retrieved surface amount (Section 4.2.2) during the 2016 Christmas event. Such an exercise should also allow an identification of those properties that yield the best match with Met-Norway snow gauge measurements at Haukeliseter.

The majority of the MASC images from Haukeliseter contained snow particles that looked like the left image Figure 4.2.1 (red frame). Such images suggest small ground-up blowing snow particles that are consistent with the high winds observed during the event. However, a careful examination of the MASC images finds the presence of rimed aggregates such as those in the right five images (Figure 4.2.1). Pristine crystals such as plates and columns were not observed during the Christmas 2016 event. As such, the use of two different aggregate particle models developed for the CloudSat mission are further investigate (Figure 4.2.1).

Figure 4.2.2 presents hourly measured snowfall accumulations on 22 December 2016 plotted against retrieved values for the two different aggregate assumptions. The 'B8' aggregate is a low reflectivity per unit mass aggregate that worked well for the cold, dry conditions observed at Barrow as described in Cooper et al. [2017]. The 'B6' aggregate, presented in Appendix A.1, is a high reflectivity per unit mass particle (Section 2.4.1). As such, the 'B6' aggregate would seem more physically consistent with the observed rimed particles (Figure 4.2.1, 5 aggregates to the right) and humid environment found in the coastal mountains at Haukeliseter. The presence of a water or rimed coating on the aggregates aloft would greatly enhance their effective reflectivity.

Indeed, Figure 4.2.2 suggests that the reflective 'B6' aggregate agree much better than the less reflective 'B8' aggregate with the snow gauge. During the Christmas storm 2016 the assumption of the 'B8' aggregate shows overestimation of precipitation amount at the ground compared to the double fence gauge for all six-days.

Table 4.2.1 presents the percentage differences between snow gauge and retrieved estimates found when using these particle model assumptions for 22 December 2016. Use of the 'B6' aggregate agreed within 5 % of the double fence observations (Table 4.2.1) for both 12 h and 24 h surface

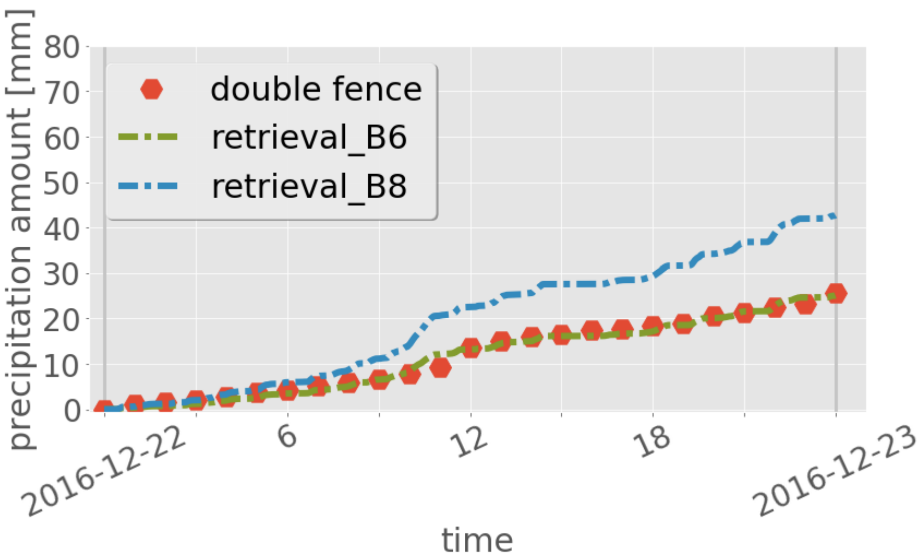

Figure 4.2.2: Hourly double fence snowfall accumulations [mm] plotted against retrieved values for the 22 December 2016 for different retrieval assumptions permutations. Double fence snowfall accumulation, red hexagons, retrieved precipitation amount for the here used study (B6), green, dash-dotted, and for small aggregates (B8), blue dashed.

accumulations. Admittedly, use of the 'B6' aggregate produced slightly too little snowfall relative to the gauges for the remaining days of the event as discussed in Section 4.2.2. The use of the 'B8' aggregate, however, overestimates snowfall by at least 65 % for both the 12 h and 24 h surface accumulations (Table 4.2.1). Since this aggregate had low reflectivity per unit mass, it required significantly more SWC in the forward model calculations (Section 2.4.1) to match MRR reflectivities. The retrieval therefore overestimates snowfall rate for these meteorological conditions at Haukeliseter during the Christmas 2016 storm.

The sensitivity study here has focused on MASC estimates of habit instead of particle size distribution or fall speed. The reason is that MASC and PIP primarily detected blowing snow particles at the surface that likely were much smaller than the particles that the MRR remotely sensed aloft. The use of the PSD measured by the MASC or PIP in the retrieval therefore produced much larger snowfall than those measured by the double fence snow gauges, e.g. on 22 December 2016 (Figure 4.2.2). Essentially, it takes a much greater mass of small particles than large particles to match a given reflectivity. The results during the Christmas 2016 event contrast with those found for low wind speed events at Haukeliseter where the use of MASC habit, PSD, and fall speed observations resulted in retrieved snowfall accumulations very close to Met-Norway double fence gauge observations. Regardless, for this high wind event, the a priori temperature PSD relationship by Wood [2011] and a climatological average fallspeed of 0.85 $\mathrm{m\,s^{-1}}$ [personal communication, Schirle, 2018] were employed. 'B6' rimed aggregate assumption resulted in a better agreement than the 'B8' assumption for surface accumulation during the Christmas 2016 storm. Therefore, the difference between the retrieved precipitation amount at the ground and the double fence gauge observations will be further studied in the following section. Conclusion for the rest of my study?

Table 4.2.1: Observations by the double fence gauge (obs.) and retrieved snowfall amounts (ret.) for 22 December 2016 for different particle model assumptions. B6 is the rimed aggregate assumption used in this thesis (Section 2.4.1) and B8 the assumption for small particles as used in the CloudSat optimal estimation snowfall retrieval.

Particle model	12 h **accumulation**			24 h **accumulation**		
	Snowfall		**Difference**	**Snowfall**		**Difference**
	obs.	**ret.**		**obs.**	**ret.**	
	[mm]		[%]	[mm]		[%]
B6	13.6	13.2	−3.0	23.1	25.1	−2.1
B8	13.6	22.5	+65.5	23.1	42.7	+66.9

4.2.2 Comparison of Surface Observations

To be able to compare the vertical predicted snow water content with the retrieved snow water content a verification of the surface accumulation is made. If the retrieved surface accumulation is reliable in comparison to the double fence measurement, then the vertical measurements can be trusted.

The correlation in Figure 4.2.3a demonstrates a good agreement between the 48 h accumulation measured by the double fence and the retrieved surface accumulation. The black line in Figure 4.2.3a presents a linear correlation with a regression coefficient of $R = 0.97$. In general, the retrieved surface snowfall accumulation is underestimated when compared to the double fence measurements, but not to a large degree.

Figure 4.2.3b shows the difference between retrieved accumulation and observed accumulation by the double fence. For the time period 21 to 24 December 2016, Figure 4.2.3b indicates an underestimation of retrieved snow accumulation of less than −5 mm for the first 24 h. Snow accumulation calculated on 23 December 2016 at 0 UTC show after 24 h an underestimation by the retrieval of up to −6.5 mm. On 24 December 2016, larger underestimation after 43 h is related to the observation of liquid precipitation on 25 December 2016 between 12 UTC to 21 UTC. On 25 December 2016 no fair comparison to the double fence measurement can be performed after 12 UTC because of the neglection of liquid precipitation when temperatures exceed 2 °C.

For the Christmas storm (21 to 26 December 2016) an average difference of 85.5 % is calculated for 12 h surface accumulation (Table 4.2.2). For longer, 24 h accumulation the average difference decreases to −4.7 % (excluding values on 25 December 2016 after 12 UTC and on 26 December 2016 after 17 UTC because of attenuation at the MRR). The daily surface snowfall accumulation difference between retrieval and observation in Table 4.2.2 show almost always a well agreement to the double fence. The only well pronounced mismatch is seen on 21 December 2016, where it measures much more than the double fence gauge (+435.8 %).

Similar to this study, Cooper et al. [2017] used a CloudSat snow particle model, PSD and fall speed from MASC observations for five snow events at Barrow, Alaska. The comparison to the weather station revealed a difference between National Weather Service observations and retrieved accumulations of −18 % for five snow events.

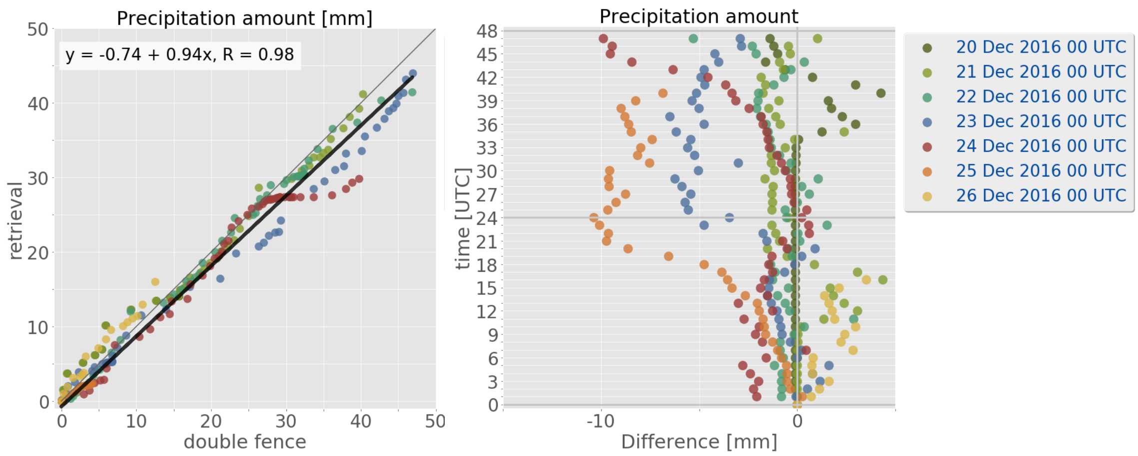

(a) (b)

Figure 4.2.3: a: Surface precipitation amount comparison between the double fence observations and the retrieved surface accumulation of precipitation for 48 h. In black the linear correlation between the double fence observations and retrieved surface snow. b: Difference between the retrieved and the observed accumulation by the double fence. The colours represent the different starting days at 0 UTC for the 48 h accumulation.

Table 4.2.2: Comparison of observed (obs.) and retrieved (ret.) snowfall amounts for the Christmas storm 2016. Difference refers to the difference of the retrieved and observed snow accumulation after 12 h and 24 h. The average difference is the value over all six/four days. Excluding values after 12 UTC on 25 December 2016 and after 17 UTC on 26 December 2016.

Day in 2016	12 h **accumulation**				24 h **accumulation**			
	Snowfall		**Difference**	**Average difference**	**Snowfall**		**Difference**	**Average difference**
	obs.	**ret.**			**obs.**	**ret.**		
	[mm]		[%]	[%]	[mm]		[%]	[%]
21 Dec	0.7	3.8	+435.8		17.1	16.6	−2.7	−4.7
22 Dec	13.6	13.2	−3.0	−2.1	25.6	25.1	−2.1	
23 Dec	6.3	5.2	−16.8		23.3	19.8	−14.9	
24 Dec	14.7	13.4	−8.6		24.8	25.0	+0.8	
25 Dec	4.3	–	–		+15.4	–	–	
26 Dec	8.8	10.6	+20.1		25.1	–	–	

Table 4.2.2 shows the difference for each individual day and the average difference for six and four days, depending on the accumulation of 12 h or 24 h. The choice of the correct PSD model, slope parameters and fall speed in the optimal estimation snowfall retrieval, shows a good agreement with the observations at Haukeliseter for the 2016 Christmas storm in contrast to the 200 % difference when only using the CloudSat snowfall algorithm (Section 2.4). It also indicates a reduction of the non-uniqueness of snow accumulation is reduced, when using a combination of ground-based observations instead of only Ze-S relationships.

It turns out that there is no relation between high and low precipitation events since the differences vary daily. Cooper et al. [2017] also showed different combinations of PSD assumptions and snow fall speed. For Barrow, best agreements between observations and retrieved snowfall were found by using the CloudSat particle model, slope parameters and snowfall speeds from the MASC. In the here presented study, the best assumption for surface snowfall accumulation was found by using a particle model for rimed aggregates (Section 2.4 and 4.2.1) such as in Figure 4.2.1.

On 21 December 2016, the deviation is large (435.8 %). This is probably related to an observation of precipitation at the double fence, while the MRR did not observe precipitation. On 21 December 2016, observation at the double fence might be related to some particles stirred up by wind into the orifice of the gauge. Since no manual observations are done at the Haukeliseter site, is it difficult to say if blowing snow occurred or if it was snowing. This introduces additional errors on the double fence measurements. From the vertical MRR reflectivity, in Section 4.2.4, Figure 4.2.7, it can be seen, that precipitation was not observed on 21 December 2016 before 9 UTC.
Even though it is assumed that the double fence is the correct measurement, there are still some uncertainties, such as under-catch during high wind speeds [Wolff, unpublished]. A better way to examine the accuracy of the retrieved surface snowfall accumulation could be to compare the results to measurements inside a bush gauge.
Wolff, [unpublished] estimates the under-catchment of double fence gauge compared to bush gauge measurements to 10 %, for outside winds of $9\,\mathrm{m\,s^{-1}}$ (Section 2.3.1). If the double fence gauge underestimate snowfall under high wind condition, would follow that the optimal estimation retrieval results are more than 20 % too low to the true state.
During the Christmas 2016 event the average difference is low for 24 h surface accumulation in Table 4.2.2 (−4.7 %). At Barrow, Alaska, the best average difference between retrieved and observed surface accumulation was 36 % [Cooper et al., 2017]. This leads to a very good agreement between observed and retrieved snow accumulation during 21 to 24 December 2016. In Section 4.2.4, the vertical SWC will be compared to the forecasted MEPS values for the 2016 Christmas storm. Despite the under-catchment of snow in high wind speeds, the double fence measurement give trust for the retrieved profiles of snow water content. While snow water content is compared to the MEPS forecast, it should be kept in mind that retrieved snow accumulation is underestimated and therefore the vertical SWC may be too low.

4.2.3 Comparison of Surface Observations and MEPS

Hereafter, MEPS surface precipitation prediction forecast is compared to the double fence gauge observations at Haukeliseter to see if observed surface accumulation was correctly predicted by MEPS.

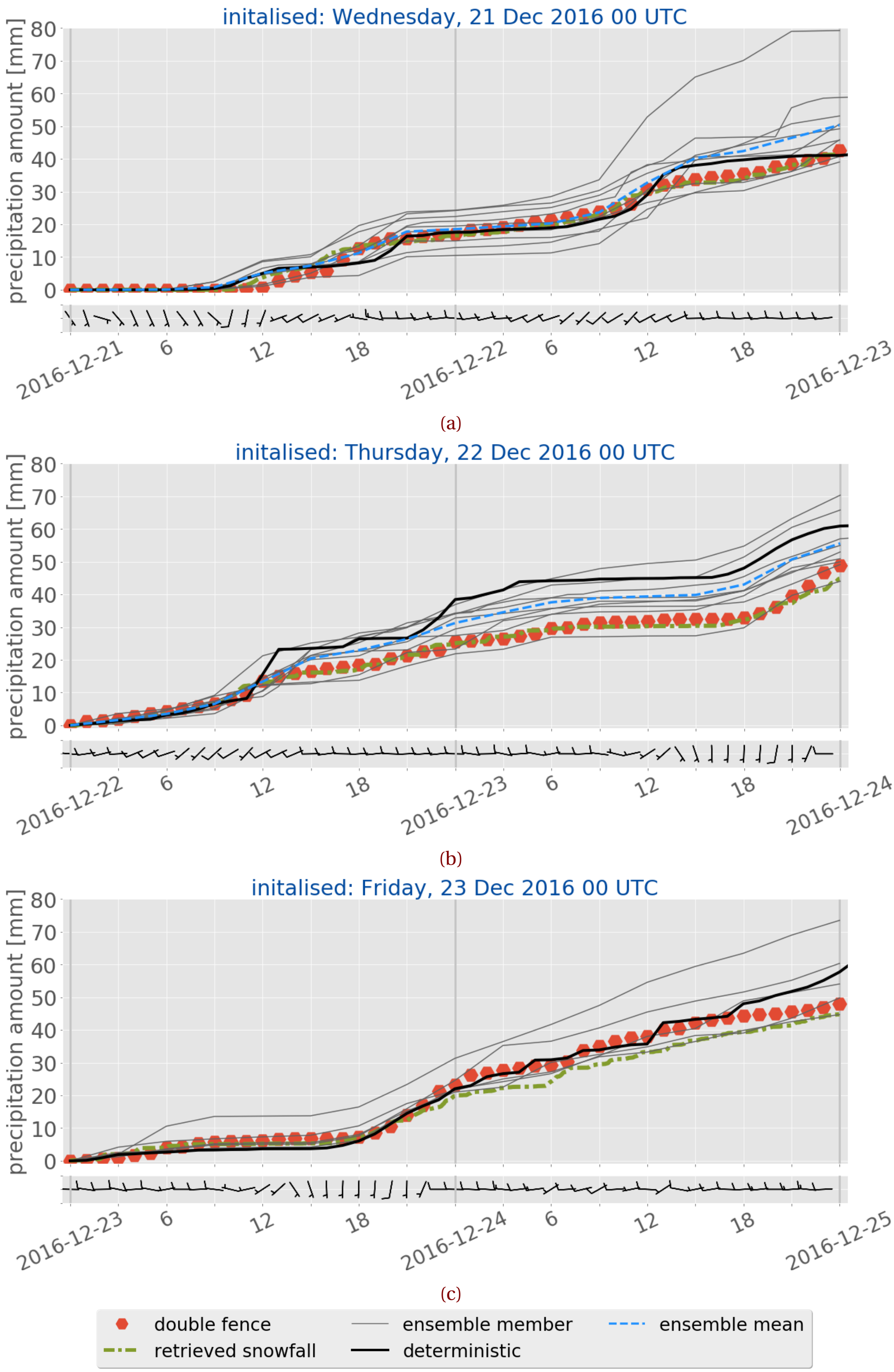

Figure 4.2.4: 48 h surface precipitation accumulation for 21 to 23 December 2016. Representing the values from the double fence in red, hexagons; optimal estimation retrieval output at the first noise free level in dash-dotted green; MEPS ensemble member deterministic forecast, initialised at 0 UTC in black and its nine perturbed ensemble members in grey. The ensemble mean of all ten members is shown in dashed blue. Underneath is the associated last hour 10 min average wind from the weather mast at 10 m height.

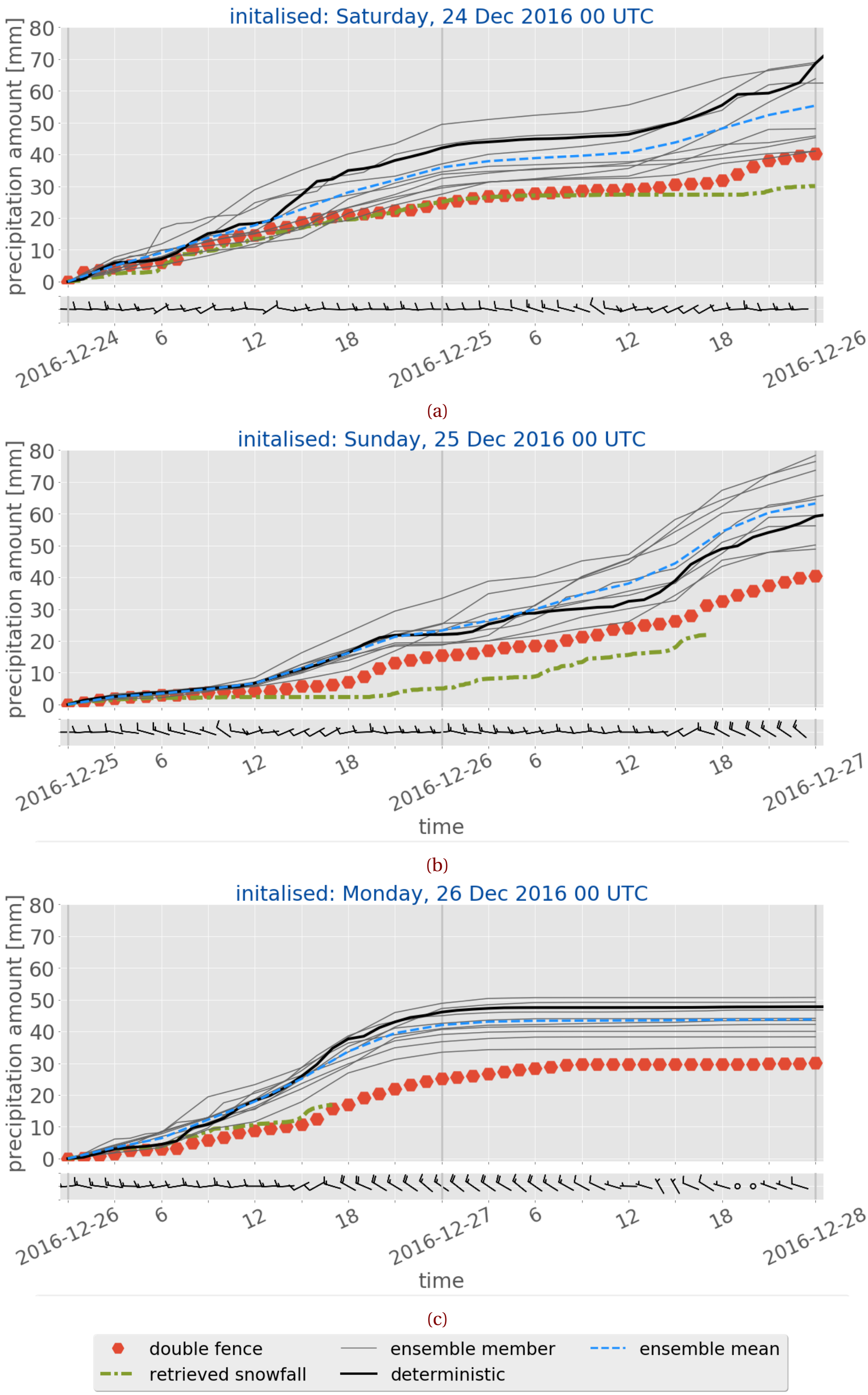

Figure 4.2.5: *(As Figure 4.2.4.)* Initialisations on 24, 25, and 26 December 2016 at 0 UTC.

?? shows surface accumulation observations at the double fence, retrieved snow accumulation, and MEPS forecast for 48 h. The blue dashed line shows the ensemble mean of all ten members. The ensemble mean of precipiation amount is calculated every three hours, due to the three hourly time resolution of most of the perturbed member (Section 2.7.1). When not all perturbed member forecast data was available from the Norwegian Meteorological Institute [2016], like on 23 December 2016 (Figure 4.2.4c), no ensemble mean is calculated. At the bottom of **??** the associated 10 min average wind of the last hour from the 10 m weather mast at Haukeliseter is presented. This will help to see if surface precipitation observations by the double fence may be influenced by wind. MEPS surface accumulation does not account for undercatchment by too high wind speeds, and therefore are not presented in **??**.

In general, Figures 4.2.4a to 4.2.4c show a better agreement between double fence precipitation amount observations and forecast for 48 h forecasts initialised on 21 to 23 December 2016 at 0 UTC than for initialisations on 24 to 26 December 2016. The double fence observation lie for 21, 22, and 23 December 2016 within the spread of the ensemble members (Figures 4.2.4a to 4.2.4c), covering the uncertainty within the measurements (Section 2.5). On the other hand, observations between 24 and 26 December 2016 are too low compared to the ensemble spread (Figures 4.2.5a to 4.2.5c). During 24 and 26 December 2016, the low-pressure system intensifies and gets closer to the Norwegian coast, influencing the local weather in Norway (Section 3.6). Figure 4.2.5a to c indicate a larger estimated surface precipitation amount for all ten ensemble members compared to observed values at the measurement site between 24 to 26 December 2016. Furthermore, all ensemble members seem to overestimate the surface accumulation after 18 h on 24 December 2016 and after 12 h on 25 and 26 December 2016.

The correlation for precipitation between 48 h double fence observation and ensemble precipitation forecast is presented in Figure 4.1.7c and d. Showing a better agreement for 21 to 23 December 2016 than initialisation on 24 to 26 December 2016. On 21 to 23 December 2016 the slope of the regression line is relatively close to unity.

Initialisations on 24 December 2016 (Figure 4.2.5a) indicate an overestimation of the deterministic surface snowfall prediction already after 13 h forecast time. The deterministic forecast in solid black in Figure 4.2.5a is much higher and increases faster than the observations and the nine perturbed members. In Figure 4.2.5a at 16 UTC, a difference of approximately 15 mm can be seen when compared to the surface measurements. This difference remains almost constant over the forecast time.

While the cyclone propagates closer to Norway, the forecast error of the surface precipitation increases. Overestimation occurs around 12 UTC on 25 December 2016. This overestimation of the precipitation amount could be associated with the warm sector evolution at Haukeliseter (Section 4.1). Afterwards, with increasing lead time MEPS forecasts show the same simulated precipitation development as the double fence, but too high. The precipitation is light between 12 UTC and 18 UTC which shows as a almost constant surface precipitation amount. At 18 UTC the surface precipitation amount at the double fence increases and so does the MEPS forecast. An overestimation of the surface precipitation is also simulated on 26 December 2016. While the

Table 4.2.3: Observations (obs.) and forecasted (MEPS) snowfall amounts for the Christmas storm 2016. Difference refers to the percentage difference between MEPS ensemble members and the double fence observation, averaged over all ensemble member for 12 h and 24 h. The average difference is the value over all days.

<table>
<tr><th rowspan="3">Day
in 2016</th><th colspan="5">12 h accumulation</th><th colspan="5">24 h accumulation</th></tr>
<tr><th colspan="2">Snowfall</th><th rowspan="2">Difference</th><th colspan="2" rowspan="2">Average difference</th><th colspan="2">Snowfall</th><th rowspan="2">Difference</th><th colspan="2" rowspan="2">Average difference</th></tr>
<tr><th>obs.</th><th>MEPS</th><th>obs.</th><th>MEPS</th></tr>
<tr><td></td><td colspan="2">[mm]</td><td>[%]</td><td colspan="2">[%]</td><td colspan="2">[mm]</td><td>[%]</td><td colspan="2">[%]</td></tr>
<tr><td>21 Dec</td><td>0.7</td><td>5.1</td><td>+626.1</td><td rowspan="3">+1.3</td><td rowspan="6">+134.7</td><td>17.1</td><td>18.5</td><td>+8.3</td><td rowspan="3">+10.8</td><td rowspan="6">+32.6</td></tr>
<tr><td>22 Dec</td><td>13.6</td><td>13.4</td><td>−1.6</td><td>25.6</td><td>31.3</td><td>+22.2</td></tr>
<tr><td>23 Dec</td><td>6.3</td><td>6.6</td><td>+4.2</td><td>23.3</td><td>23.7</td><td>+1.8</td></tr>
<tr><td>24 Dec</td><td>14.7</td><td>17.7</td><td>+20.4</td><td rowspan="3">+59.8</td><td>24.8</td><td>35.9</td><td>+44.8</td><td rowspan="3">+54.4</td></tr>
<tr><td>25 Dec</td><td>4.3</td><td>6.7</td><td>+55.1</td><td>15.4</td><td>23.3</td><td>+50.8</td></tr>
<tr><td>26 Dec</td><td>8.8</td><td>17.9</td><td>+104.0</td><td>25.1</td><td>42.1</td><td>+67.5</td></tr>
</table>

surface analysis indicates the passage of an occlusion after 15 UTC (Figure 3.6.7a, 3.6.7c, and Section 4.1). The overestimation seems to occur after a 12 h lead time in Figure 4.2.5c. The MEPS ensemble seems to predict the timing of precipitation correctly compared to the double fence, but estimates a too high surface accumulation. Table 4.2.3 shows the difference between the observations and ensemble mean MEPS forecast for 12 h and 24 h accumulation. As seen in Table 4.2.3, the average difference decreases with longer forecast time. For 21 to 26 December 2016 the deviation is +134.7 %. For longer lead times, 24 h, the average difference is reduced to +32.6 %. Generally the forecast accuracy decreases with lead time [Kalnay, 2003]. On 21 December 2016 very large deviation (626.1 %) is shown. AROME-MetCoOp had problems with too low precipitation. The deviation between observed and forecasted values was larger if the precipitation amount is less than 10 mm [Müller et al., 2017]. At Haukeliseter, low precipitation amount is observed (0.7 mm) on 21 December 2016. The daily percent difference show to be high for the last three days of the 2016 Christmas extreme event.

The largest overestimation of MEPS forecast for precipitation amount is seen in Table 4.2.3 on 26 December 2016 with +104 % for 12 h. This shows the highest overestimation for the three days (24 to 26 December 2016).

In Figure 4.1.9 show the ensemble member a balanced bias from 21 to 23 December 2016. The bias for 24 to 26 December 2016 is wet, also showing the overestimation of surface accumulation. In Figure 4.1.10e, the mean absolute error is less than 7 mm for 21 to 23 December 2016 and increases with intensification of the storm up to 14 mm on 26 December 2016. The mean absolute error in Figure 4.1.10e for 12 h precipitation is less than 7 mm on 25 December 2016, similar to 21 to 23 December 2016.

Since MEPS performance was better on 21 to 23 December 2016 one might assume that the double fence measurement is influenced by surface winds. Wolff, [unpublished] states that the double fence gauge is influenced by wind, and that the double fence gauge underestimates precipitation accumulation within 10 % for winds up to 9 m s^{-1}. A relation between high wind and double fence observation could be possible. Table 4.2.4 presents the percentage difference between the double

Table 4.2.4: Same as Table 4.2.3, adjusted just for an under-catchment of 10 % difference by the double fence gauge.

<table>
<tr><th rowspan="3">Day in 2016</th><th colspan="5">12 h accumulation</th><th colspan="5">24 h accumulation</th></tr>
<tr><th colspan="2">Snowfall</th><th>Difference</th><th colspan="2">Average difference</th><th colspan="2">Snowfall</th><th>Difference</th><th colspan="2">Average difference</th></tr>
<tr><th>obs.</th><th>MEPS</th><th></th><th colspan="2"></th><th>obs.</th><th>MEPS</th><th></th><th colspan="2"></th></tr>
<tr><td></td><td colspan="2">[mm]</td><td>[%]</td><td colspan="2">[%]</td><td colspan="2">[mm]</td><td>[%]</td><td colspan="2">[%]</td></tr>
<tr><td>21 Dec</td><td>0.8</td><td>5.1</td><td>+553.5</td><td rowspan="3">−8.8</td><td rowspan="6">+111.2</td><td>19.0</td><td>18.5</td><td>-2.5</td><td rowspan="3">-0.3</td><td rowspan="6">+19.3</td></tr>
<tr><td>22 Dec</td><td>15.1</td><td>13.4</td><td>−11.4</td><td>28.4</td><td>31.3</td><td>+9.9</td></tr>
<tr><td>23 Dec</td><td>7.0</td><td>6.6</td><td>-6.2</td><td>25.9</td><td>23.7</td><td>-8.4</td></tr>
<tr><td>24 Dec</td><td>16.3</td><td>17.7</td><td>+8.4</td><td rowspan="3">+43.8</td><td>27.6</td><td>35.9</td><td>+30.3</td><td rowspan="3">+39.0</td></tr>
<tr><td>25 Dec</td><td>4.8</td><td>6.7</td><td>+39.6</td><td>17.1</td><td>23.3</td><td>+35.8</td></tr>
<tr><td>26 Dec</td><td>9.8</td><td>17.9</td><td>+83.6</td><td>27.9</td><td>42.1</td><td>+50.8</td></tr>
</table>

fence and MEPS forecasts under the condition that the double fence is affected by wind with a catch-ratio less than 10 %. Here, it also shows an increase in forecast accuracy for precipitation accumulation over 24 h. The average difference is reduced by 23.5 % for 12 h accumulation. Assuming an accumulation underestimation of 10 % would lead to a reduction of overestimation to 43.8 % for 12 h during 24 to 26 December 2016 (Table 4.2.4). This shows that even a 10 % under-catchment from the double fence gauge, MEPS would still overestimate the surface accumulation (12 h: +43.8 %; 24 h: +39 %).

On 24, 25, and 26 December 2016 winds between 5 $\mathrm{m\,s^{-1}}$ and 20 $\mathrm{m\,s^{-1}}$ were observed (Figure 4.1.2d, d, **??**). The accumulation after 12 h lead time in Table 4.2.4 indicate if wind may have influenced the catchment of the double fence and effect the result of overestimation. It shows, overestimation would still be present on 25 and 26 December 2016. On the other hand, overestimation would not be present for 24 December 2016 until 12 h accumulation.

Still, an simulation of too much surface accumulation is apparent for 24 h lead time. It seems even though the double fence gauge is influenced by wind, the overestimation of surface accumulation by MEPS is still present.

In order to quantify the statistical uncertainty of the ensemble members, a box-whisker plot is provided in Figure 4.2.6. The box-whisker-plots in Figure 4.2.6 show the time evolution of the distribution of the precipitation amount made of ten ensemble members up to 48 h on 24, 25, and 26 December 2016 (Figures 4.2.6a to 4.2.6c). Figure 4.2.6 provides information every 3 h, since some ensemble member do not have forecast values every hour.

All three days with overestimation seem to have different variability between the ensemble member. As expected the forecast uncertainty increases with longer forecast time for precipitation amount. Figure 4.2.6b and c show a smaller ensemble member variability on 25 and 26 December 2016 than on 24 December 2016.

Large variability is already present after 3 h prediction time in Figure 4.2.6a on 24 December 2016. The spread between the ensemble members (shown by the minimum and maximum whiskers) seems to be wide indicating a large uncertainty of the amount of surface accumulation. The ensemble mean (red line) is always higher than the median, suggesting a positively skewed distribution. After 12 h forecast time, the median is closer to the lower 25th percentile, indicating a

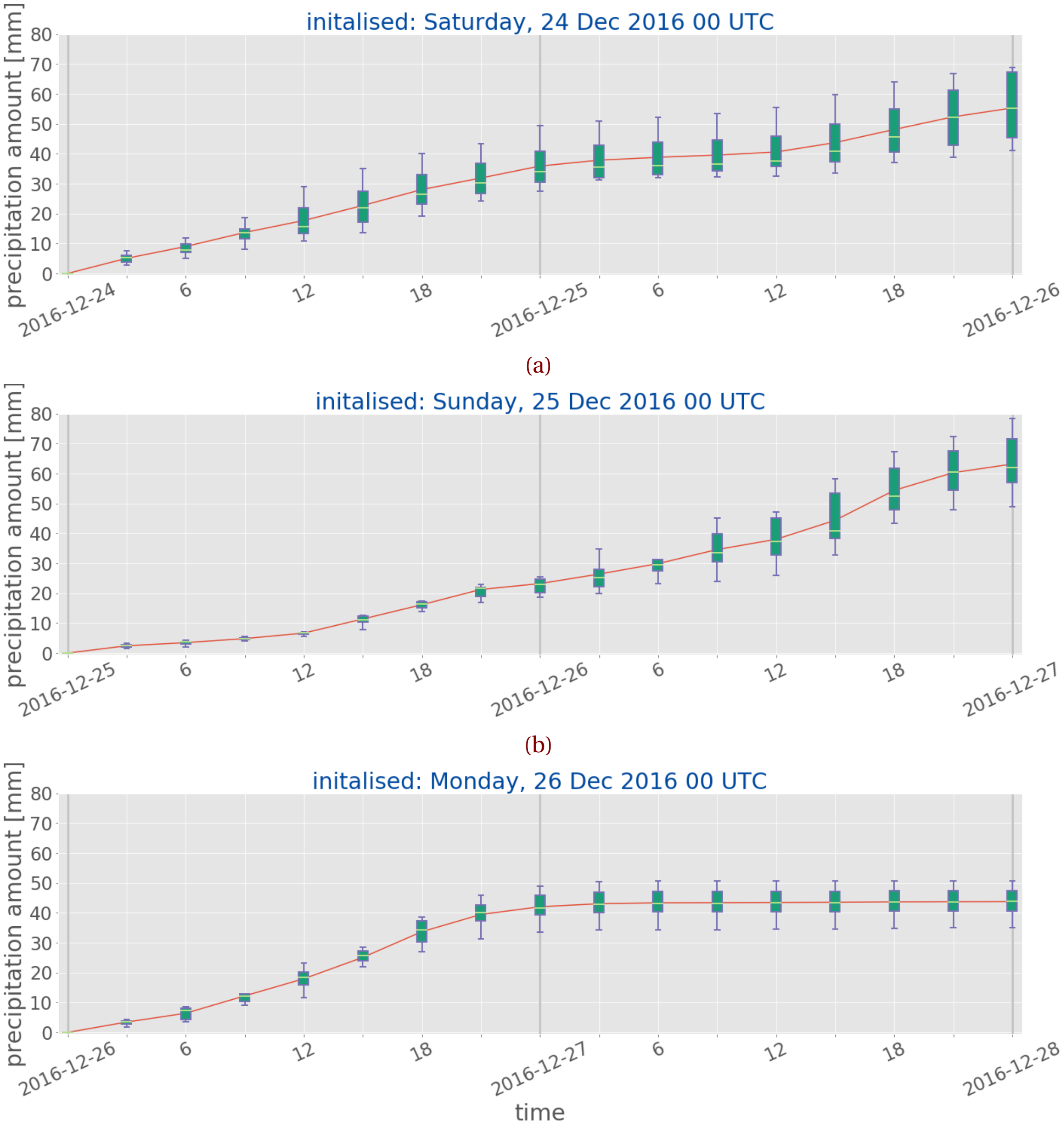

(a)

(b)

(c)

Figure 4.2.6: Box-whisker-plot in order to quantify the statistical uncertainty of the ten ensemble members of MEPS. The red line shows the ensemble mean of all ten members and if the distribution is skewed. The short light green, horizontal line is showing the median, the wide vertical box represent the 25th and 75th percentiles, and minimum and maximum values are indicated by the vertical lines, whiskers.

negative skewness. Also, all upper whiskers in Figure 4.2.6a are longer than the lower ones, which would follow that the ensemble members vary amongst the most positive quartile and that it is very similar for the least positive quartile group.

The variability in Figure 4.2.15 show no large variation between the ensemble members (narrow box-whiskers) on 25 December 2016. This day is also the forecast with the smallest wet bias of 5 mm on the three days with overestimation (Figure 4.1.9e). This may be related to the small variability between the ensemble members in Figure 4.2.6b. The variability in the forecast increases after 15 h prediction time. Median and mean agree well for the entire period of a 48 h lead time. After 39 h the mean is much higher than the median and closer to the lower 25th percentile in Fig-

ure 4.2.6b. It seems, that all ten ensemble members agree well on the prediction and nevertheless MEPS overestimates the surface accumulation.
On 26 December 2016 the highest deviation to the double fence observations is estimated (Table 4.2.4). The precipitation amount forecast is overestimating at 12 UTC in Figure 4.2.5c. Figure 4.2.6c indicates increasing variability after 6 h, but the variability between the ensemble members is not as large as on 24 December 2016 after 12 h lead time. Nevertheless, agree the ensemble member the least about the precipitation amount at 12 UTC. The spread between the ensemble members is wide showing the uncertainty. As Figure 4.2.5c also shows is the double fence observation not within the spread of the ensemble member after 9 h lead time. According to Müller et al. [2017] strong precipitation events are better predicted with AROME-MetCoOp than with ECMWF. In Section 2.2 it was described, that during 21 to 27 December 2016 56.9 % of the total December 2016 accumulation of precipitation were observed. The extreme 2016 Christmas event follows to be a strong precipitation event. The overestimation at the surface could be related to the 10 % under-catchment by the double fence gauge under high wind condition. As Table 4.2.4 indicates the difference between the forecast system and the double fence observations is decreased, but still too much surface accumulation is estimated by MEPS. The difference for 12 h lead time on 25 and 26 December 2016 is however more than 40 %. Only a 10 % under-catchment by the double fence is assumed in this thesis. This value is approximated by Wolff, [unpublished] from measurement sites for wind speed below 9 $\mathrm{m\,s^{-1}}$. Wolff, [unpublished] states that estimates for higher wind speeds such observed at Haukeliseter do not exist but is believed to be within 20 %. During the event the wind was less than 20 $\mathrm{m\,s^{-1}}$ and the forecast error could be reduced because of the wind related effect of the double fence.

The uncertainty of the surface accumulation might also have been related to the fact that the large-scale situation intensified more than low pressure systems in Norway usually do.
The overestimation on 24 December 2016 can be related to the high precipitation amount in the evening of 23 December 2016. The precipitation amount associated with the transition of the occluded front on 23 December 2016, after 18 UTC, is higher than on previous days (Figure 4.2.4c and Figure 3.6.4e). During 20 to 21 December 2016, the hourly precipitation around 0 UTC is less intense than on 23 December 2016 (Figure 3.6.4e). High accumulation amount over shorter time followed and could have resulted in a larger variability of the MEPS members (Figure 4.2.6). In the analysis cycle 3 h prior the initialisation of MEPS observations are included inside the model domain [Homleid and Tveter, 2016]. Since the precipitation amount associated with the occlusion passage on 23 December 2016 was quite high, might this have led to the overestimation of surface precipitation amount. [Homleid and Tveter, 2016]
Another possibility is that MEPS might have accounted for more precipitation around 12 UTC on 24 December 2016 than was observed. This could show the large predicted precipitation amount in Figure 4.2.5a at 13 UTC.
On 25 December 2016 MEPS surface forecasts suggest that MEPS did not expect the occurrence of a warm front (Figures 4.1.3a to 4.1.3d). However, from the surface accumulation prediction it could be concluded that MEPS expected more precipitation around 12 UTC on 25 December 2016.

Maybe MEPS has expected a weak warm-front passage and therefore more precipitation. The fact that the temperature is rising and therefore the phase is changing from snow to liquid precipitation (Figure 4.1.8) may have led to MEPS expecting more liquid precipitationhence MEPS predicted more surface accumulation.
On 26 December 2016 between 15 UTC and 18 UTC, the core of the Christmas 2016 low-pressure system passes over Haukeliseter (Figures 4.1.4a to 4.1.4d). Overestimation of surface accumulation are seen after 12 UTC in Figure 4.2.5c. It is very likely that overestimation on 26 December 2016 is related to passage of the low pressure system, since ensemble prediction systems are not adjusted to predict perfectly for extreme events.

Observations are used as initial condition in weather forecast systems, such as MEPS. As described in Section 2.5, should the observations be within the spread of the ensemble member prediction. Furthermore, the forecast members should be close together for a short time, so they may be considered *deterministic*. This is not the case for 24 to 26 December 2016 after 12 h lead time.
Uncertainties appearing already after 3 h and 6 h on 24 and 26 December 2016 could be associated with a long spin-up time of MEPS. As described in Section 2.5, MEPS precipitation has a spin-up time of 6 h and values before that should not be used as very certain [Køltzow, 2018, personal communication]. Even though this is taken into account, Figure 4.2.6 show larger variability for the ensemble members on 24 and 26 December 2016 after 6 h prediction.
As a result of poorer initial conditions the spin-up time could have been longer on 24, 25, and 26 December 2016. The spin-up time can vary due to less or also uncertain observations going into the initialisation [Warner et al., 1997]. Observations are fed into MEPS directly by using the operational global forecast model ECMWF, which initialises observations. Less observations can be due to instrumentation failure or the data has not been transmitted in time to the forecasting system [Kalnay, 2003]. Observations have errors and this can increase the initial uncertainty in a weather forecast. The atmosphere is a chaotic system and it depends sensitive on initial conditions [Lorenz, 1969]. Longer spin-up time than the usual 6 h for precipitation can lead to larger variation from early on in Figure 4.2.6a and c than e.g. on 25 December 2016. More variability between the ensemble members does not necessarily mean that a forecast is bad, it only shows the predictability.
Since the box-whisker-plot in Figure 4.2.6b (25 December 2016) show less variability in the beginning it is assumed that spin-up time issues are less likely, but not totally excluded. It could be related to an error in the initialisation, even though it does not show within the variability at the beginning.

The overestimation of accumulated precipitation during 24 and 26 December 2016 might be related to local horizontal resolution of MEPS at Haukeliseter as well as to the complex development of the low-pressure system north-west of Norway on 24 December 2016.
Generally, ensemble prediction forecast systems are overall performing best during usual large-scale weather situations. The studies from Buizza et al. [1999], Petroliagis et al. [1997] show that

the ECMWF ensemble prediction can be extremely beneficial for assessing the forecast skill during extreme precipitation events.
It is more likely that the overestimation of precipitation amount was more related to the local topography and the strong winds observed during the intensification of the extreme event. As well as the orographic representation in the regional model MEPS. Effects of the topographical resolution on MEPS at Haukeliseter, will be further discussed in Section 4.2.5.

4.2.4 Comparison of Snow Water Content in the Vertical

Frontal passages were observed at the surface several times throughout the extreme storm in December 2016. MEPS is able to predict the large scale synoptics and related precipiation, temperature, and wind changes for initialisation more than 24 h in advance (Section 4.1). Three additional instruments were installed to measure snowfall up to 3 km at Haukeliseter.

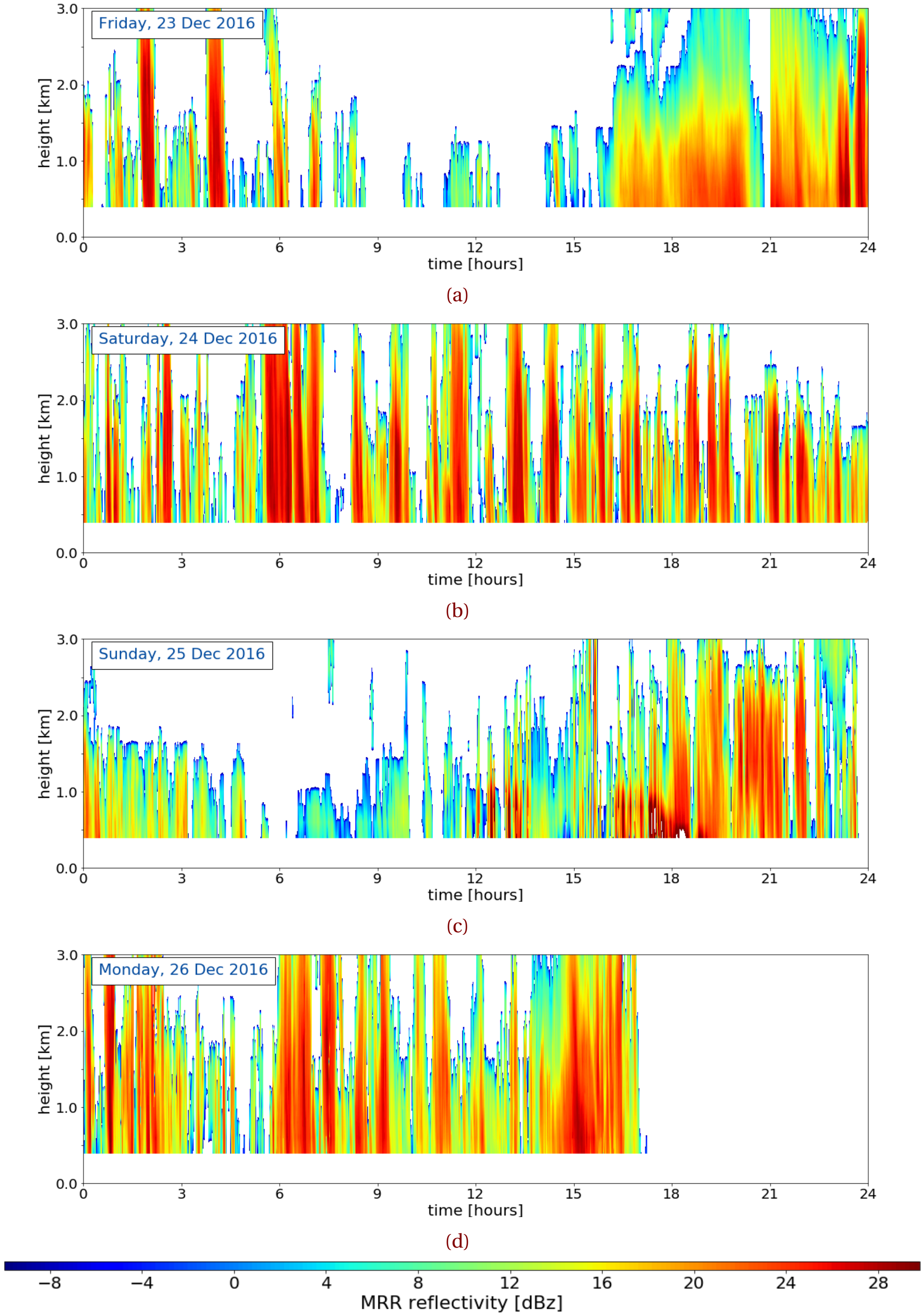

Figure 4.2.7: MRR reflectivity for the days with frontal passage and overestimation at the ground at Haukeliseter. dBZ reflectivity according to the colour bar, with weaker precipitation in blue and more intense precipitation in red. a: Friday, 23 December 2016, b: Saturday, 24 December 2016, c: Sunday, 25 December 2016, and d: Monday, 26 December 2016.

This gives the opportunity to compare the forecasts with retrieved vertical snow water content

(Sections 4.2.1 and 4.2.2). As far as the author is aware of there is no study about verification of vertical ensemble member prediction models with observations.
Previous studies such as Joos and Wernli [2012] motivate to make accurate surface measurements more available to improve mesoscale models.
Passages of occluded fronts and a warm sector were observed on 23, 26, and 25 December 2016. Additionally, an overestimation at the ground is shown on 24, 25, and 26 December 2016 for surface precipitation amount (Section 4.2.3, **??**).

Figure 4.2.7 shows the reflectivity from the MRR at Haukeliseter for these days. Likely periods of snowfall are inidcate with orange and red in Figure 4.2.7.On 26 December 2016 only values until 17 UTC are displayed, because of the temperature change and hence a precipitation shift led to liquid drops freezing on the MRR dish so that the signal got attenuated.
More stable flow pattern with high reflectivity values in Figure 4.2.7 indicate the transition of the occlusion on 23, 26, and the warm sector passage on 25 December 2016. The high reflectivity on 23 and 26 December 2016 shows the passage of the occlusion and the associated frozen precipitation. On 23 December 2016, the surface observations of sea level pressure (Figure 4.1.2a), 2 m air temperature (b), and 10 m wind (c), allow to assume that the occluded front passed through Haukeliseter between 12 UTC and 21 UTC. Figure 4.2.7a shows high observed reflectivity in the lower up to 3 km at Haukeliseter after 16 UTC. After 16 UTC, the wind is from the south, upslope (Figure 4.1.2c, Figure 2.1.1c) which led to a moderate precipitation pattern in Figure 4.2.7a. In the morning of 23 December 2016 high amount of frozen precipitation was observed at 2 UTC and 4 UTC, but with a more disturbed pattern than in the evening.
Another occlusion passed through on 26 December 2016 between 15 UTC and 21 UTC (compare surface observations Figure 4.1.4a to e). An uninterrupted precipitation pattern and high reflectivity in Figure 4.2.7d indicate the passage after 15 UTC. While on 23, 24, and 26 December 2016 the reflectivity did not pass values larger than 28 dBZ, Figure 4.2.7c shows high reflectivity values larger than 30 dBZ on 25 December 2016 (compare for approximation Table 2.3.1). These high reflectivity values up to 1.2 km in Figure 4.2.7c indicate the observation of possible liquid precipitation on 25 December 2016. Images from the MASC were able to verify observed liquid drops during 12 UTC to 21 UTC (Figure 4.1.8). In the observations on 25 December 2016, high temperatures (Figure 4.1.3b) are shown, between 12 UTC to 21 UTC. On 24 December 2016 short, interchangeable high and low reflectivity patterns are present in Figure 4.2.7b. **??** and **??** indicate strong wind from the west which led to a more disturbed precipitation structure in Figure 4.2.7b on 24 December 2016. The same pulsing is seen on 26 December 2016 before 12 UTC in Figure 4.2.7d. A comparison with the observed surface wind in Figure 4.1.4c and d shows also westerlies. The orographic influences on the surface wind and therefore a possible relation to the precipitation patterns will be further investigated in Section 4.2.5.

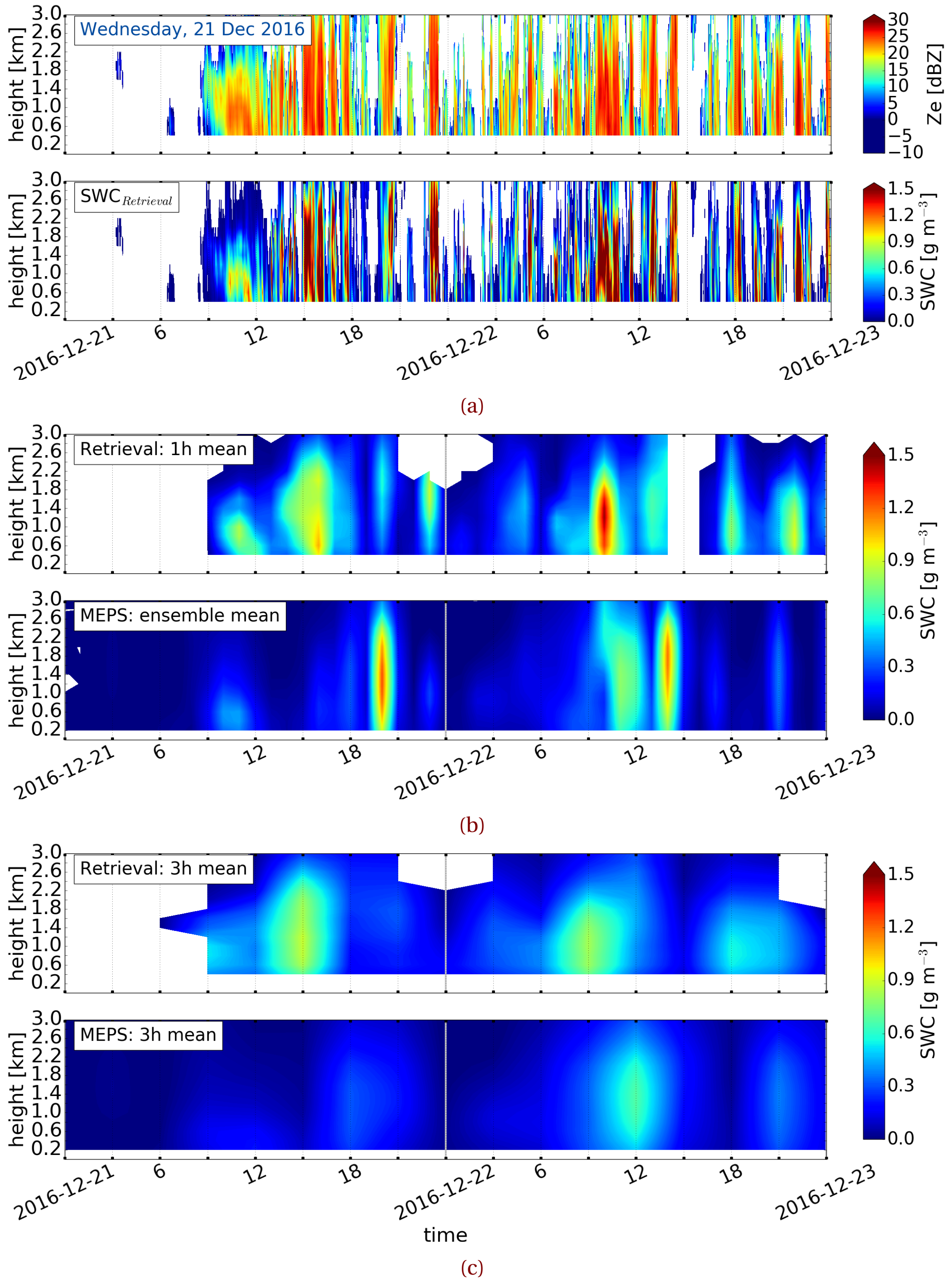

Figure 4.2.8: Initialisation on 21 December 2016 at 0 UTC. From top to bottom: (a) MRR reflectivity for 48 h, minutely retrieved SWC. (b) Hourly averaged retrieved SWC, lower panel instantaneous hourly averaged forecast of all ensemble member SWC, neglecting missing values. (c) Three hourly averaged retrieved SWC, lower panel instantaneous three hourly averaged forecast of all ensemble member SWC.

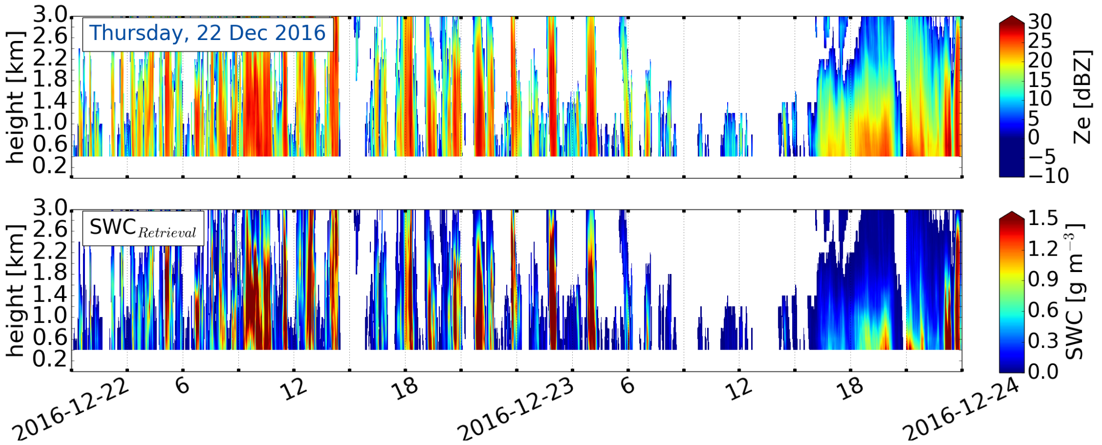

(a)

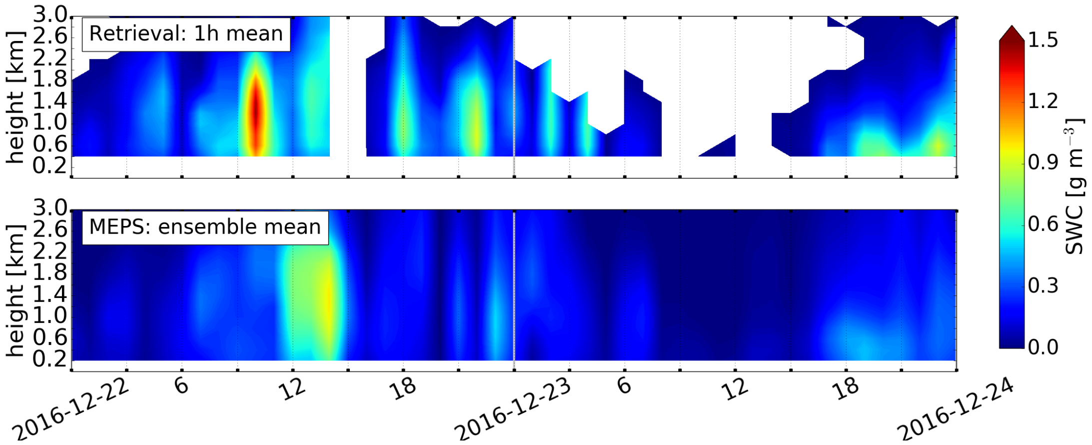

(b)

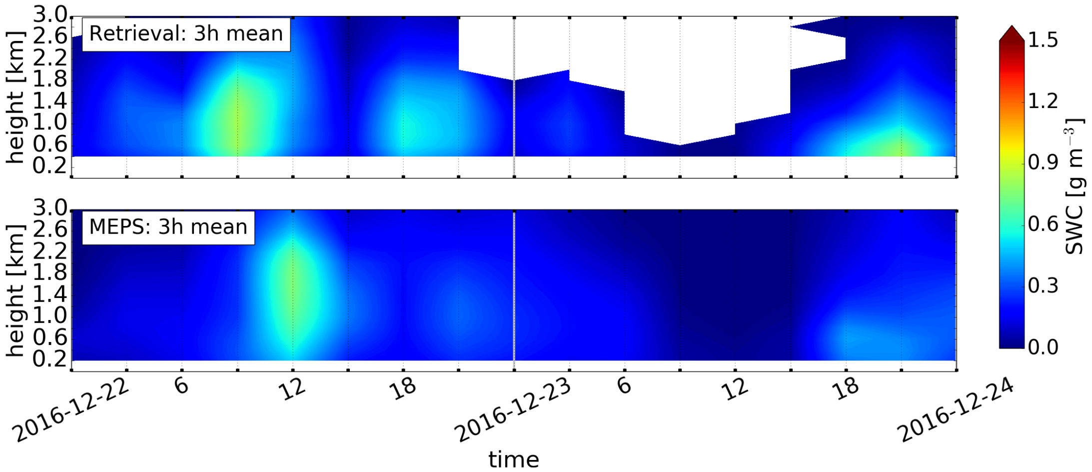

(c)

Figure 4.2.9: *(As Figure 4.2.8.)* Initialisation 22 December 2016 at 0 UTC.

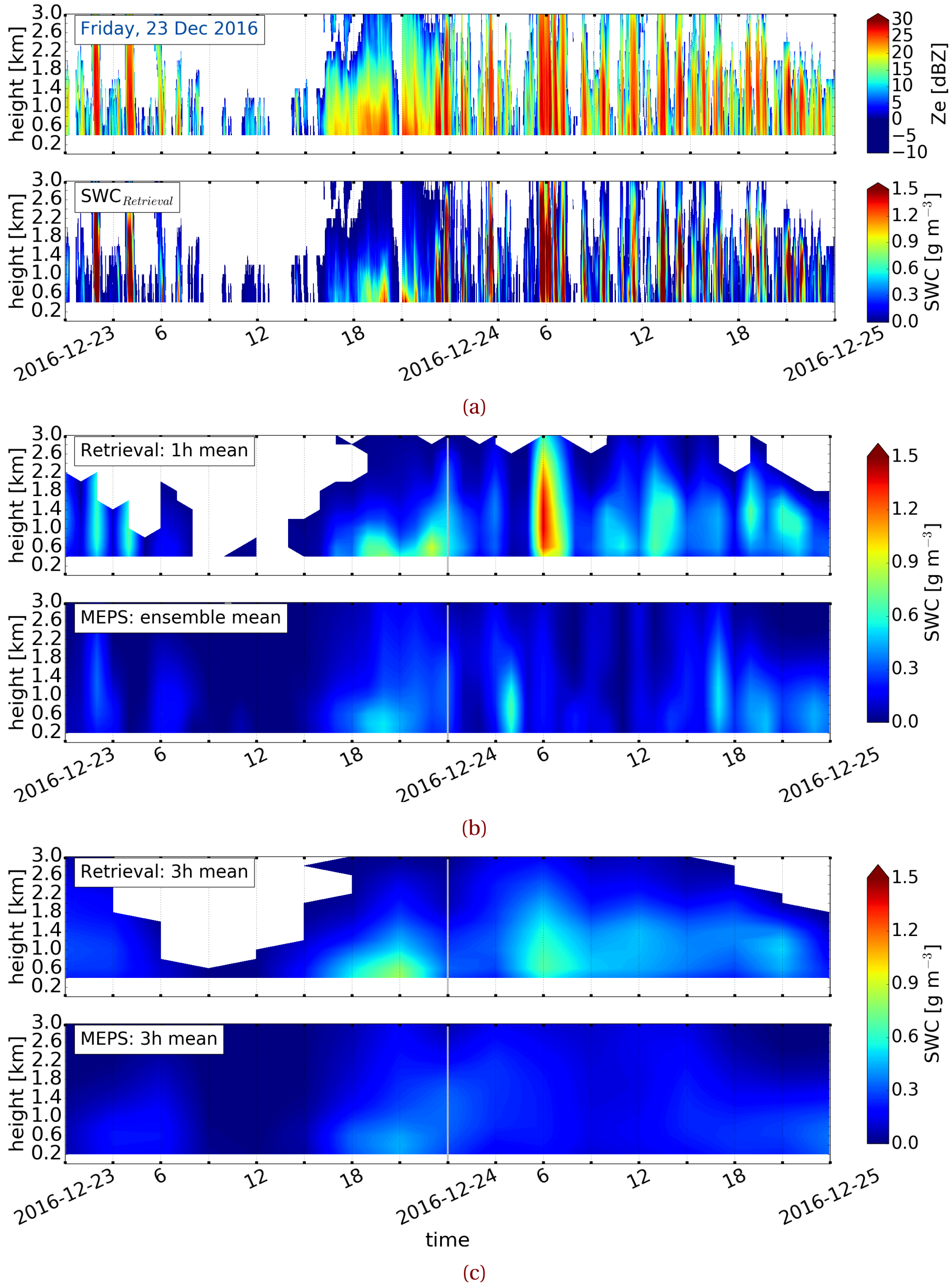

Figure 4.2.10: *(As Figure 4.2.8.)* Initialisation 23 December 2016 at 0 UTC.

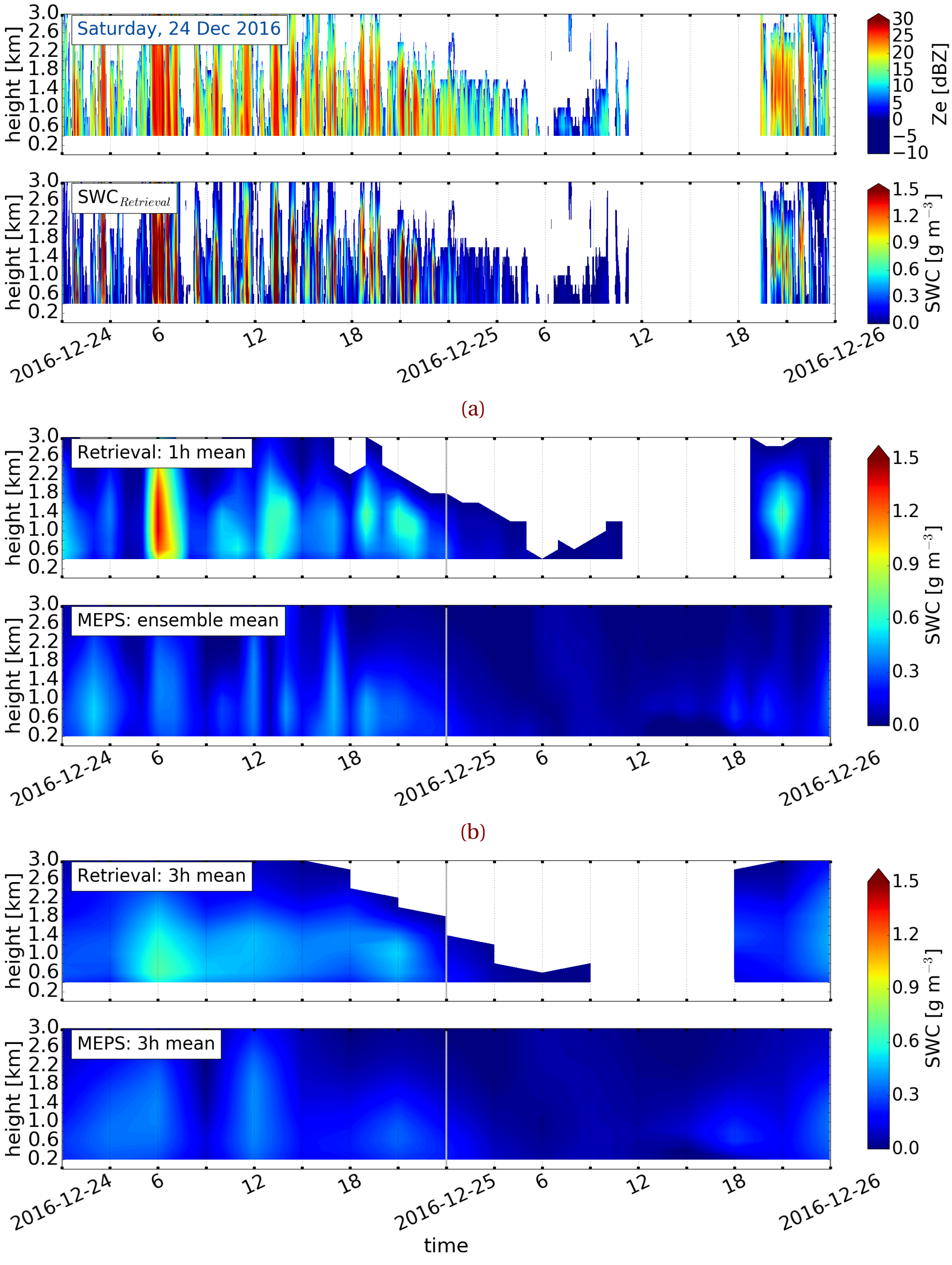

(a)

(b)

(c)

Figure 4.2.11: *(As Figure 4.2.8.)* Initialisation 24 December 2016 at 0 UTC.

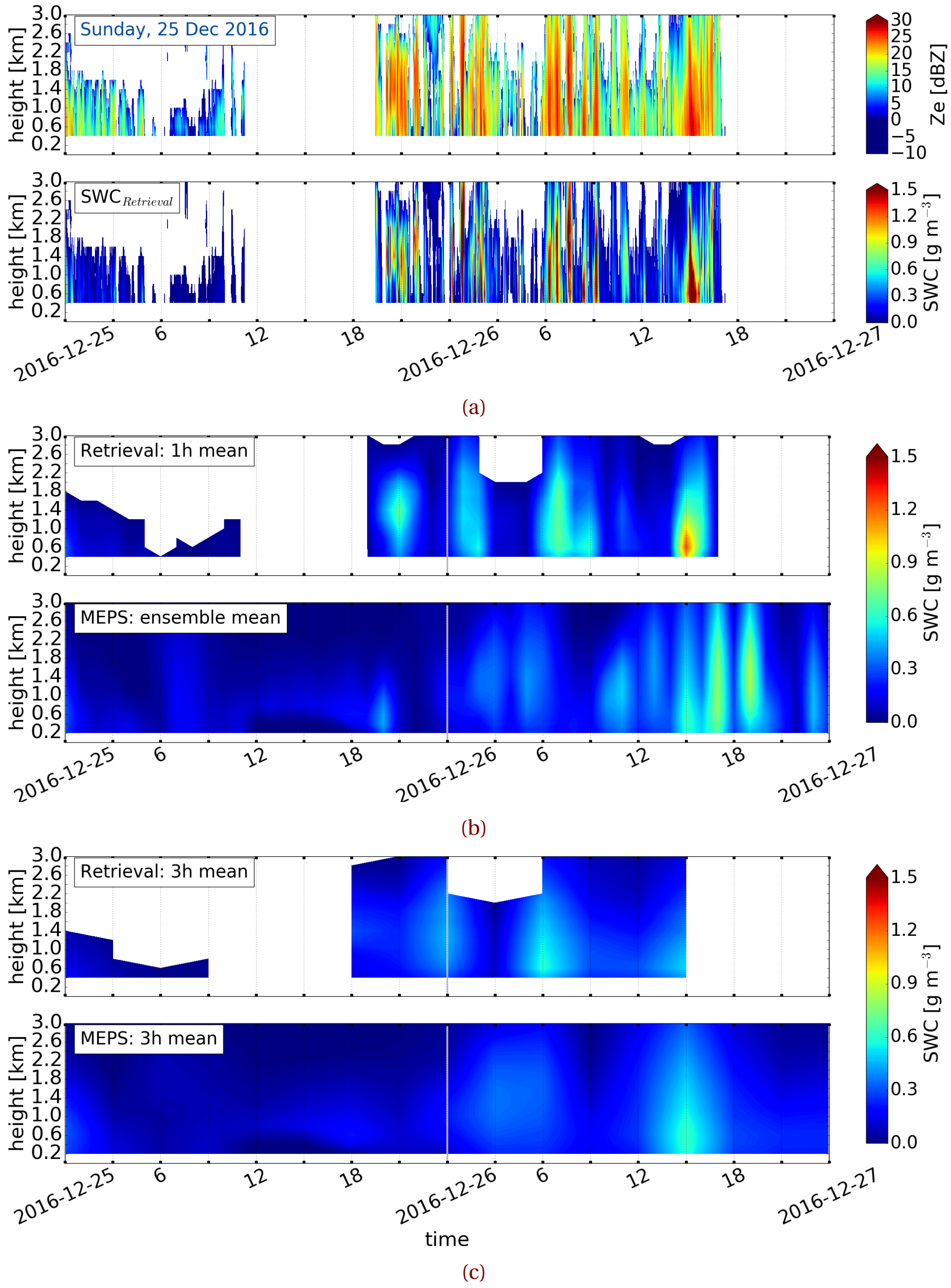

Figure 4.2.12: *(As Figure 4.2.8.)* Initialisation 25 December 2016 at 0 UTC.

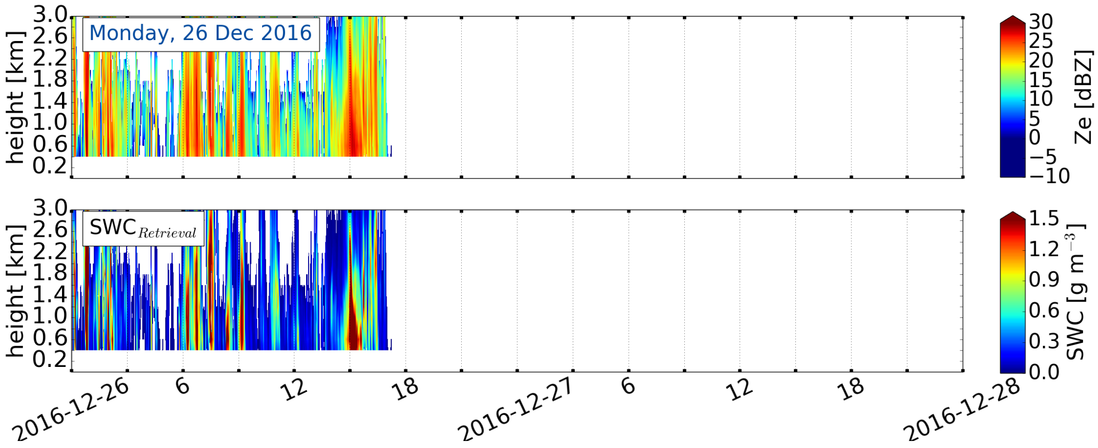

(a)

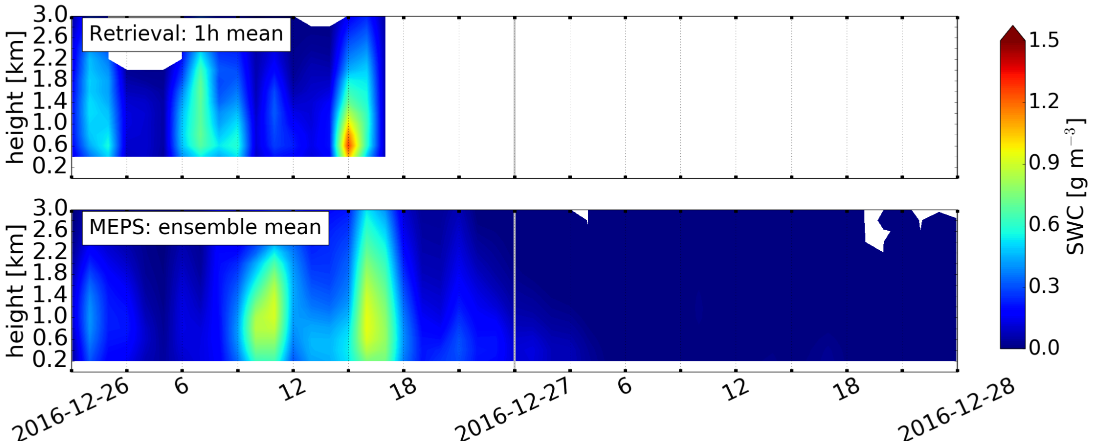

(b)

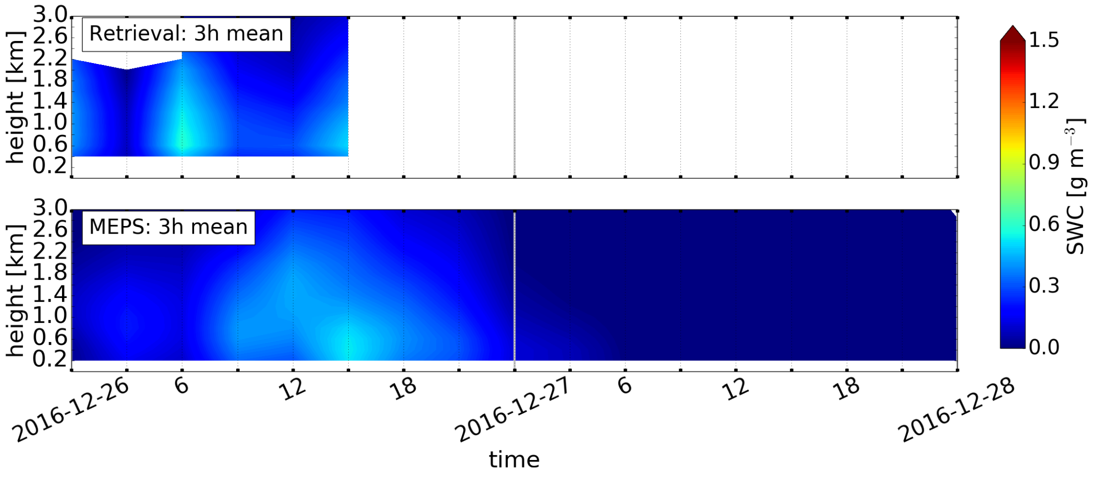

(c)

Figure 4.2.13: *(As Figure 4.2.8.)* Initialisation 26 December 2016 at 0 UTC.

Figures 4.2.9 to 4.2.13 present the reflectivity of the MRR and the snow water content retrieved from the reflectivity as well as the 48 h forecast values. Minutely MRR reflectivity and retrieved snow water content can be seen in Figure 4.2.9a to 4.2.13a. Figure 4.2.9b to 4.2.13b show in the upper panel the hourly averaged values from the retrieved SWC and in the lower panel the ensemble mean of the instantaneous forecast values every hour over all ensemble member. Three hourly averaged retrieved values are then presented in the upper panel of Figure 4.2.9c to 4.2.13c, the

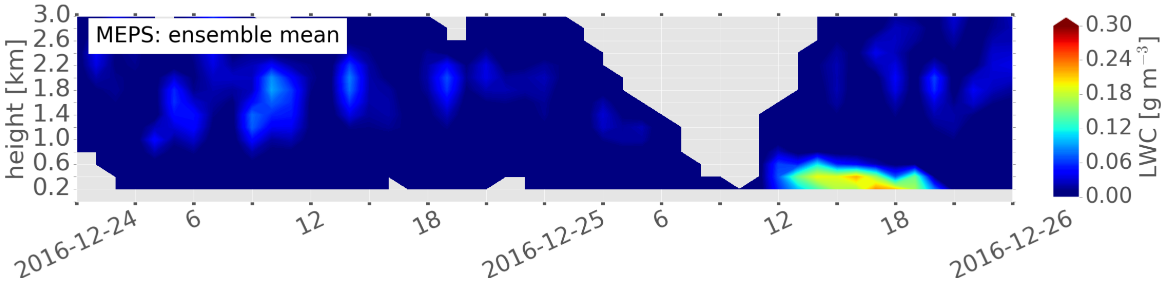

(a)

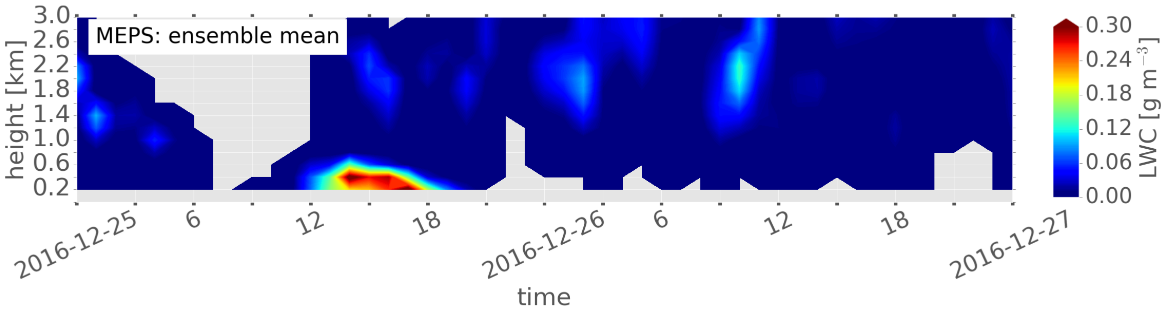

(b)

Figure 4.2.14: Ensemble mean 48 h MEPS forecast for liquid water content. The Liquid water content is averaged over a layer thickness of 200 m. Missing values are neglected. Liquid water content according to the colour bar. Initialised on 24 December 2016 and 25 December 2016 at 0 UTC.

lower panel are the ensemble mean forecast values every three hours. On 23 December 2016 an occlusion passes over Haukeliseter between 16 UTC and 23 UTC. The passage of the occlusion on 23 December 2016 is already predicted for initialisations on 22 December 2016 in Figure 4.2.9b, c. With shorter lead time the snow water content for hourly and three hourly ensemble means increases in Figure 4.2.10b and c after 16 UTC on 23 December 2016. MEPS is able to estimate the snow water content for ensemble means of time resolutions 3 h in Figure 4.2.9c, 4.2.10c.
On 26 December 2016, retrieved snow water content until the passage of the occlusion is observed (Figures 4.1.4a to 4.1.4e). The average of all ensemble members (Figure 4.2.13b) as well as the three-hourly instantaneous SWC (Figure 4.2.13c) predict the frontal transition between 15 UTC and 21 UTC. Initialisations already 39 h prior (25 December 2016) let assume that intense precipitation will occur over a short time (Figure 4.2.12b, c).
In general, the 25 December 2016 was a very weak snow storm with liquid precipitation observed between 11 UTC and 19 UTC in Figure 4.2.7c. The retrieved snow water content in Figure 4.2.11 and 4.2.12 show a gap of missing values during liquid precipitation (Section 2.4.2). The initialisations on 24 (Figure 4.2.11) and 25 December 2016 (Figure 4.2.12) show forecasted snow water content less than 0.4 g m^{-3} for 25 December 2016 while the retrieved maximum value is 0.7 g m^{-3} at 15 UTC.
To see if liquid precipitation is predicted, the atmospheric cloud condensed water content and rainfall amount in model levels is summed (Figure 4.2.14). Figure 4.2.14a and b show liquid water content for initialisations on 24 December 2016 and 25 December 2016, respectively. Positive surface temperatures are forecasted between 12 UTC and 21 UTC (Figure 4.1.3b). Initialisations more than 24 h prior (24 December 2016) show already the occurrence of the liquid precipitation

Table 4.2.5: Interpretation of the coefficient of variation for SWC.

Size of CV [%]	**Interpretation** variability
0 to <25	negligible
25 to <50	low
50 to <75	moderate
75 to <100	high
100 to ∞	very high

layer (Figure 4.2.14a). Figure 4.2.14a and b show also a narrow liquid layer thickness up to 800 m for initialisations on 24 and 25 December 2016.
In Norwegian mountainous terrain this is an important forecast ability, since precipitation change can lead to a high risk for people. The avalanche danger increases with the precipitation change especially during high wind speeds [Hansen et al., 2014]. A change from snow to liquid precipitation increases the risk of transport accidence because of freezing rain. Since MEPS forecasts the liquid layer correctly in thickness and duration it seems to be a good interaction between the surface model temperature and the temperature assimilation. This follows a high accuracy of MEPS for liquid forecast and the positive impact of using a high resolution convective scheme model.

The hourly comparison between all ten ensemble members is not fair. Therefore, an ensemble mean is created only with the deterministic and first perturbed ensemble member. Averaging only the deterministic and first ensemble member forecast leads to little snow water content in Figure B.1.1. Figure B.1.1b, c and e, f show no occurrence of occlusion passages on 23 and 26 December 2016, respectively. Furthermore, the pulsing on 24 December 2016 is seen weak for initialisations on 24 December 2016 (Figure B.1.1d), but not 48 h prior.
A comparison with each individual ensemble member shows high instantaneous values of 1.5 $\mathrm{g\,m^{-3}}$ for the deterministic and first ensemble member (Figure B.2.1). This is seen for initialisations on almost all days during the Christmas event.
Surface overestimations were seen on 24, 25, and 26 December 2016 (Section 4.2.3). Higher predicted SWC for the deterministic and first perturbed member might have led to an overestimation of surface accumulation seen in Figures 4.2.5a to 4.2.5c (for ensemble member zero and one). A comparison with the other days show the same result, when only the deterministic forecast and first perturbed member is used Figure B.1.1.

The variation of each initialised ensemble member for snow water content is given in Figure B.2.1 for the respective day. One possibility to quantify the variability of all ensemble member during the Christmas 2016 storm, is by calculating the coefficient of variation (CV) for SWC, described in Section 2.7.1. Figures 4.2.15b to 4.2.15e show the coefficient of variation for SWC and gives the possibility to compare the SWC for different days with each other. The interpretation of the coefficient of variation for SWC is presented in Table 4.2.5.
The grey line in Figure 4.2.15 presents the ensemble mean of the hourly predicted SWC values. The

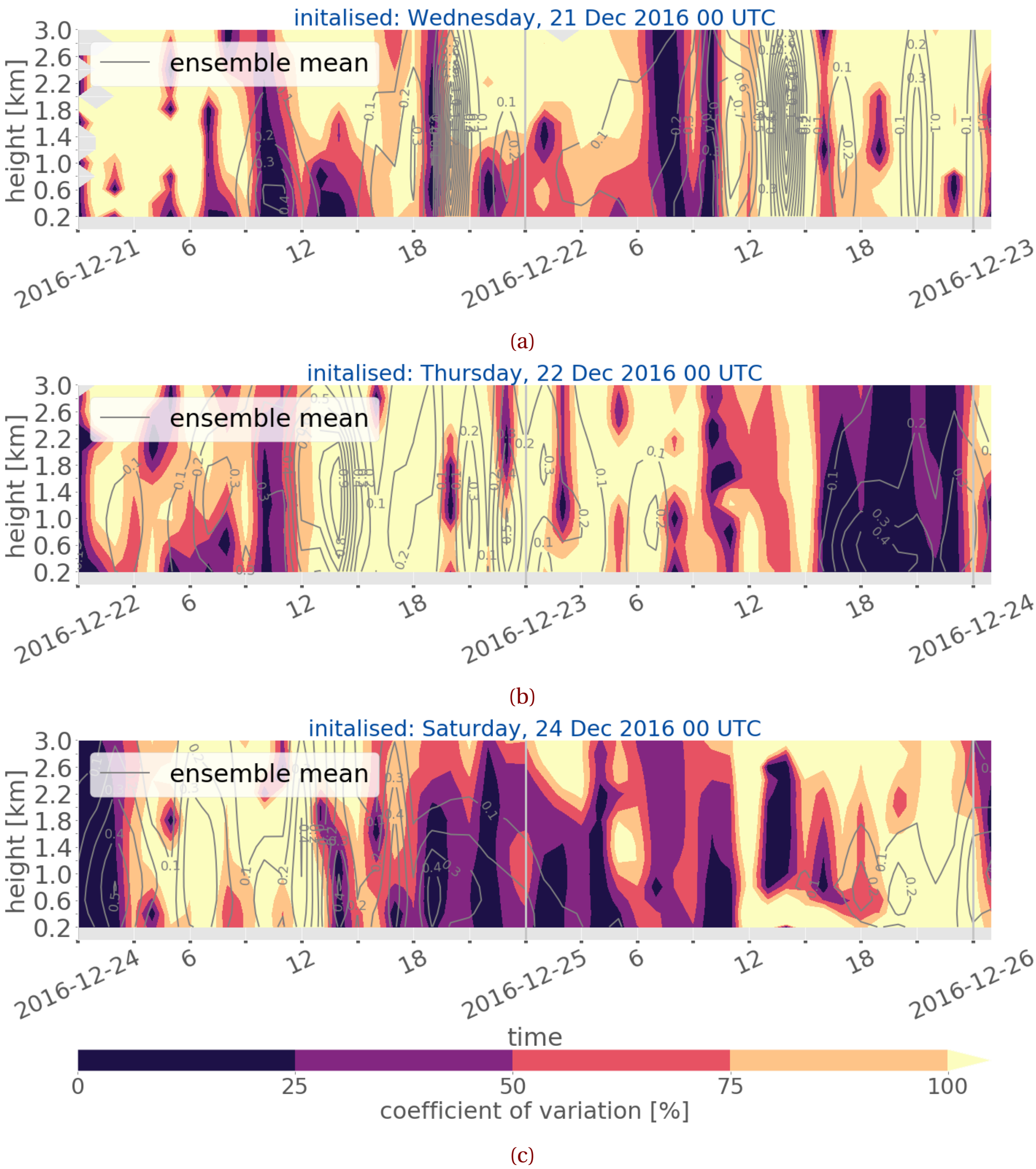

Figure 4.2.15: SWC variation of the ten ensemble members of MEPS. The lighter the colour according to the colour bar the higher the variation between the perturbed ensemble members. In grey the ensemble mean of all ten members. For initialisations on 22 and 24 December 2016. *Continued on next page.*

darker the shading in Figure 4.2.15 the smaller the variation of the SWC relative to the mean. MEPS data does not exist for all ten ensemble members on 23 December 2016. No coefficient of variation is calculated for this day, since only six perturbed members were available. Therefore, the initialisation on 22 December 2016 is used to validate the forecast. On 23 December 2016, two intense SWC pulses are observed in the lower troposphere at 2 UTC and 4 UTC (Figure 4.2.10a). The deterministic forecast, initialised on 22 December 2016 predicted a peak at 1 UTC and 3 UTC, where the first perturbed ensemble member (EM1) has a strong SWC at 3 UTC. Initialisations 24 h later show only one peak in the deterministic forecast at 2 UTC.

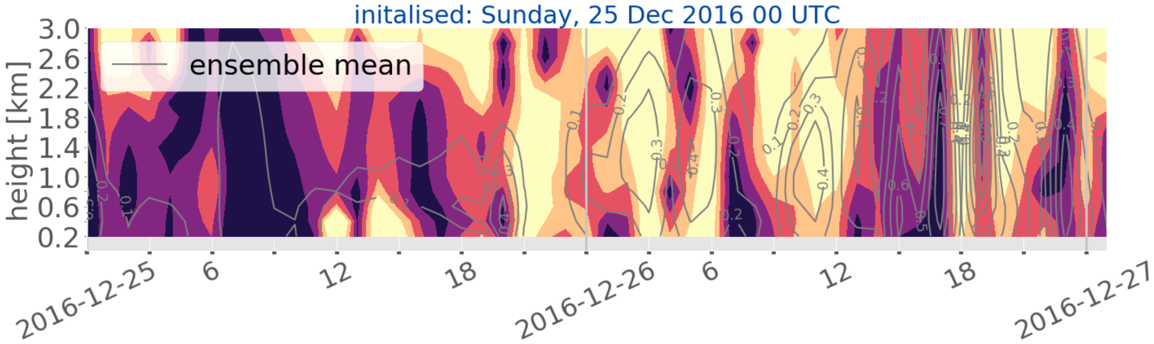

(d)

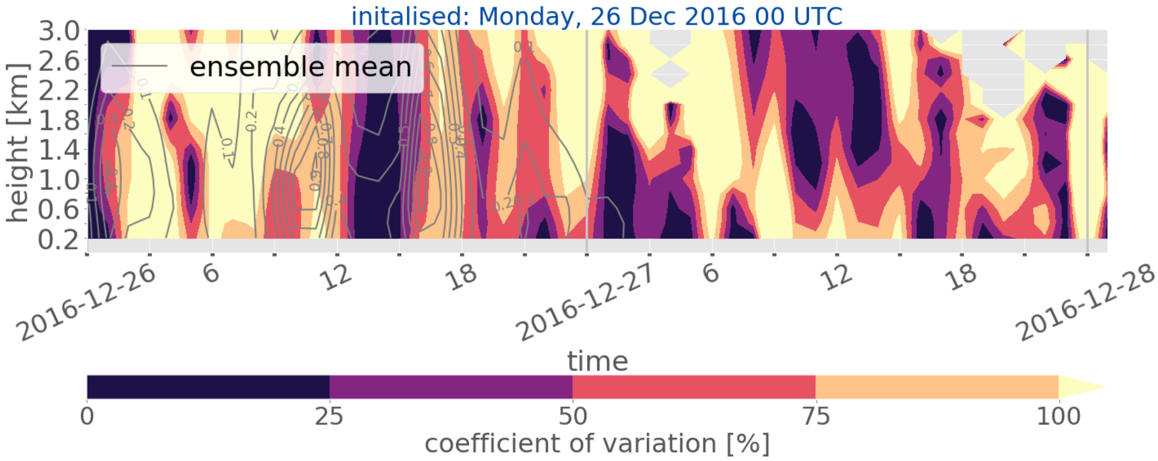

(e)

Figure 4.2.15: *(Continued from previous page.)* Initialisation 25 and 26 December 2016.

The occlusion passage on 23 December 2016 is seen after 16 UTC in Figure 4.2.10. Initialisations on 22 December 2016 (Figure B.2.1b) show for each ensemble member a weak predicted snow water content for the transition of the occlusion. No MEPS forecast data was available for four perturbed ensemble for initialisations on 23 December 2016. The comparison of only six ensemble members in Figure B.2.1c, let assume that the variability between all ensemble members during the up-slope storm is low.Nevertheless, for initialisations on 22 or 23 December 2016 all ten ensemble members forecast the uninterrupted precipitation pattern to occur after 16 UTC (Figure B.2.1b and c). For prediction initialised on 22 December 2016 the verification in Figure 4.2.15b shows little variability below 50 % and show a good agreement on the occurrence of snow fall after 16 UTC. Before 16 UTC a disturbed SWC pattern is observed in the lower 3 km at Haukeliseter on 26 December 2016. All ten ensemble member in **????** predict pulsing patterns. Initialisations on either 25 or 26 December 2016 show interchangeable precipitation for the deterministic and first ensemble member similar as the retrieved snow water content (Figure 4.2.13).
The surface observations for 26 December 2016 indicate the passage of the occlusion at Haukeliseter between 15 UTC and 19 UTC (Figures 4.1.4a to 4.1.4d). A larger variability than for the occlusion passage on 23 December 2016 (Figure 4.2.15b) between the ensemble members is shown for the evolution of the occlusion on 26 December 2016 in Figure 4.2.15d, e.
Initialisations on 25 December 2016 present a lower variability for the transition of the occlusion after 15 UTC on 26 December 2016 (Figure 4.2.15d) than initialisations less than 24 h prior (Fig-

ure 4.2.15e). Therefore, an increase of variability for shorter lead time is given in Figure 4.2.15e. The variation of all members for initialisations on 25 December 2016 (Figure B.2.1e) and on 26 December 2016 (B.2.1f) indicate that almost all perturbed member would have predicted the precipitation after 16 UTC on 26 December 2016, but the ensemble mean (Figure 4.2.12, **??**) weakens the result.

Initialisations on 25 December 2016 (Figure 4.2.12b, c) would suggest a continues pulsing of the storm after the occlusion passage. The two peaks around 18 UTC (Figure 4.2.12b) are predicted with a negligible and moderate variability in **??**. The retrieved snow water content in Figure 4.2.13b shows a peak at 1 UTC. Initialisation on 26 December 2016 forecast a high snow water content around 1 UTC as well. The forecasted SWC peak at 1 UTC is related to a moderate variability of the ensemble members (Figure 4.2.15e). Initialisations on 25 and 26 December 2016 show high forecast variability for the predicted SWC between 9 UTC and 12 UTC. The peak between 15 UTC and 18 UTC has a low to moderate variability between the members. When looking at Figure B.2.1f might this disagreement be related to the variation of the vertical predicted SWC. There seems to be no agreement between the different members about the incidence of the different SWC peaks on 26 December 2016. The high conflict for the CV before noon is most likely related to the high SWC of the deterministic SWC.

On 25 December 2016 forecasts for the warm sector passage show liquid precipitation (Figure 4.2.14). Initialisations on 24 December 2016, indicate very low forecast variability up to 0.8 km until noon, this is when liquid precipitation was forecasted by MEPS and observed (Figure 4.1.8). The depth of the liquid layer is up to 0.8 km in Figure 4.2.14a and 4.2.14b. The variation coefficient for snow water content (Figure 4.2.15c and 4.2.15d) has a large disagreement below 0.8 km, because of a low predicted SWC in Figure 4.2.11, **??**. Above 0.8 km the variability for snow water content between the members is low. Initialisation on 24 December 2016 show weak snow water content peak in Figure 4.2.11b and c at 18 UTC, which had a moderate variability (Table 4.2.5, Figure 4.2.15c). Afterwards it is very high. Initialisation on 25 December 2016 show low forecast variability until noon (Figure 4.2.15d). While liquid precipitation is predicted the variability in the lower layer is first very high and shortly before 18 UTC not existing. A high agreement for the SWC peak at 20 UTC up to 0.8 km exists in Figure 4.2.15d and decreases to be moderate above. Oscillating snow water content patterns are seen for the individual ensemble member forecasts for initialisations on 24 December 2016 (**??**). On 24 December 2016 the observed snowfall in the lower troposphere changed between intense and less intense (Figure 4.2.11).

This is not a fair comparison since hourly instantaneous values are used and there might be a time delay of half an hour about the development of boundaries which would follow it is not seen in the model forecast. As well as the best agreement is reached for ensemble means of all ten ensemble member at every hour.

The forecasted instantaneous snow water contentis weaker than the retrieved values for predictions during the 2016 Christmas storm.For the first glance MEPS snow water content forecast operates well when compared to observed snow water content up to 3 km and shows similar precipitation patterns. The average of all ten ensemble members leads to a weaker ensemble mean

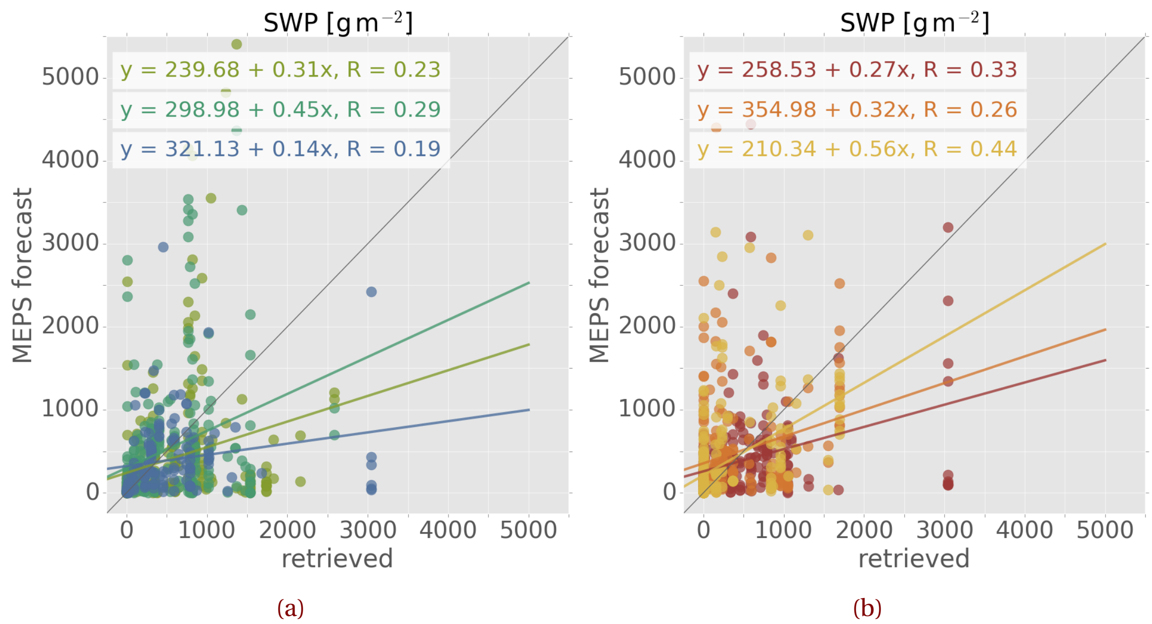

Figure 4.2.16: Snow water path correlation between retrieved and forecasted values for 48 h lead time and all ensemble member. Separated for 21 to 23 December 2016 (a) and 24 to 26 December 2016 (b).

for hourly or three hourly instantaneous values in **????????????**. To compare if lower snow water content was predicted than retrieved from the optimal estimation retrieval the snow water path is calculated (Section 2.6.3).

Figure 4.2.16 shows the correlation between retrieved and individual ensemble member 48 h forecasted snow water path (SWP). The correlation coefficient is for the days of the Christmas storm less than 0.45 $\mathrm{g\,m^{-2}}$ indicating a weak uphill correlation between retrieved and predicted values. For all days, the slope of the regression line is smaller than 1 $\mathrm{g\,m^{-2}}$. This shows, retrieved values are larger than the instantaneous ensemble member forecasts for snowfall.

On 24, 25, and 26 December 2016 the surface snow accumulation is overestimated by MEPS (Figures 4.2.5a to 4.2.5c). This overestimation is not seen in the vertical. It might be related to the use of hourly instantaneous values in the vertical whereas the surface precipitation amount is the accumulated total precipitation at each hour.

Furthermore, it could be related to the interaction between the vertical model forecast and the surface forecast. Also, the optimal estimation retrieval fall speed is assumed to be constant (0.85 $\mathrm{m\,s^{-1}}$, Section 2.4.1) whereas in MEPS the terminal speed velocity is assumed to be related to the particle diameter (Equation (2.5.6)).

One question to answer in this work is, if the operational model MEPS simulates large scale phenomena correctly. As discussed here and in Section 4.1 it seems that the model is able to resolve the development of large scale and its associated precipitation. Even with the intensification of the Christmas 2016 storm MEPS seem to be able to predict extreme events for vertical snowfall such as occlusions and liquid precipitation related to warm sectors.

MEPS also distinguishes realistically between liquid and solid precipitation in strength and dura-

tion for the lower most atmosphere in mountainous terrain in Norway like Haukeliseter. This can be a major challenge since a change in temperature and associated precipitation transformation can lead to high risk in the Norwegian mountains, especially during winter.
The here presented results are a first look, trying to compare a mesoscale ensemble member forecast system (MEPS) with vertical in-situ measurement for snowfall.
The next section will go into detail, how the local orography at Haukeliseter may influence frozen precipitation, and how MEPS's representation of the topography may affect patterns of snowfall.

4.2.5 DISCUSSION

The Haukeliseter site is exposed to high wind speeds during the winter. The previous results in Section 4.1, 4.2.3, 4.2.4 have shown, that wind plays an important role for the precipitation catchment at Haukeliseter. The mountain plateau is surrounded by higher mountains to the west and more open to the south east (Figure 4.2.17a). Figure 4.2.17a presents the local topography around Haukeliseter and Figure 4.2.17b shows the 2.5 km grid resolution of the topography by MEPS. MEPS is able to cover some of the complex structure around the site (Figure 4.2.17b), with the higher mountain to the west and the valley to the south-east (Figure 4.2.17a). Haukeliseter is at an altitude of 991 m above sea level (Section 2.1). In this thesis the closest grid point to the Haukeliseter measurement site is used, which is 59.80° N, 7.22° E. The altitude of this grid point is 1041 m above sea level.

The orography influences the vertical precipitation pattern. Westerlies produce disturbed, pulsing patterns with changing intense and less intense snowfall e.g. 24 December 2016 (Figure 4.2.11). An uninterrupted structure is seen when the wind is south-easterly (up-slope) e.g. on 21 between 9 UTC and 12 UTC (Figure 4.2.8) or 23 December 2016 after 15 UTC (Figure 4.2.10).

Figure 4.2.18 shows the observed 10 m wind during the 2016 Christmas storm. It shows westerly wind is stronger up to 20 $\mathrm{m\,s^{-1}}$ at Haukeliseter. Measured south-easterlies reach wind speeds less than 8 $\mathrm{m\,s^{-1}}$.

The correlation between observations and forecast show an overestimation of predicted wind speed throughout the event (Figure 4.2.19).Müller et al. [2017] already mentioned the bias of too strong wind speed prediction in AROME-MetCoOp.

The complex terrain and its representation in MEPS might have led to the overestimation of surface precipitation amount. Alternatively, the use of four close grid points around Haukeliseter can be useful to inspect the spatial variability of surface accumulation. An average of the grid points surrounding the Haukeliseter site could lead to a solution that is closer to the truth and must be evaluated further.

Observed south-easterly winds are channelled along the valley. MEPS resolves it in the way that the wind is south-westerly. Figure 4.2.17b displays a high mountain to the west of the station and a small one to the south. The 10 m wind is predicted to blow between these two elevations in MEPS. On 21 and 23 December 2016 wind directions from the south-east (Figure 4.1.1c) and south (c) were observed, respectively. As earlier discussed in Section 4.1 and 4.2.4, the wind change is associated with the occlusion passage on 23 December 2016 (Figure 3.6.4). The wind direction change on 21 December 2016 in Figure 4.1.1c was also related to the large scale synoptic flow but is not associated to a frontal boundary (Figure 3.6.2). A comparison with the available large scale weather analysis map from ECMWF (Section 3.6), shows that the large scale surface wind is from the south-west at 6 UTC on 21 December 2016 (Figure 3.6.2c) and has changed to west at 12 UTC (Figure 3.6.2d). The observations at the Haukeliseter site show between 6 UTC and 12 UTC wind from south-east, while the predicted MEPS wind direction is from south in Figure 4.1.1c. The local wind direction influenced the precipitation pattern in the vertical on 21 and 23 December 2016. On both days, weak, south-easterly wind is observed and predicted and led to an undisturbed precipitation pattern between 9 UTC and 12 UTC on 21 (Figure 4.2.8) and after15 UTC on 23 December 2016

(Figure 4.2.10). The precipitation is not as intense than for more turbulent precipitation structure e.g. after 15 UTC on 21 December 2016 (Figure 4.2.8a).
Both days (21 and 23 December 2016) show a moderate precipitation with not as intense snow water content than for storm patterns from the west such as on 24 December 2016 (Figure 4.2.11). The forecast model seems to forecast the wind direction overall well, only on 21 December 2016 before 10 UTC is a south-west instead of a south-east wind predicted by MEPS (Figure 4.1.1c). It displays even if the large scale wind is from the south-west (Figure 3.6.2d) the local wind is rather from the south or south-east (Figure 4.1.1c). This small scale effect is most likely associated to the topography around Haukeliseter (Figure 4.2.17).
Figure 4.1.6d shows a good correlation for west winds, but on the other side, southerly winds seem to be troublesome to predict for MEPS. Figure 4.1.6c indicates an inbalance for south-westerly winds. While south-easterly winds (along the valley) are observed at Haukeliseter MEPS predicts the 10 m wind to be south-westerly. As the precipitation profiles in Figure 4.2.8a, 4.2.9a, 4.2.10a, 4.2.11a, 4.2.12a, and 4.2.13a show, are westerlies associated with high snow water content. In comparison undisturbed precipitation patterns related to south-easterlies have less intense snow water content. Connection to surface Figure 4.2.19

As Figure 4.2.8b indicates the model is able to cover almost the exact timing of the up-slope storm pattern on 21 December 2016. The variability of each ensemble member initialised on 21 December 2016 is presented in Figure B.2.1a. It shows that almost all ensemble members agree on the occurrence of the storm pattern during 9 UTC to 12 UTC.
Wind from the west and therefore over high mountains (1500 m) always follow a pulsing with more intense vertical precipitation e.g. on 24 December 2016, Figure 4.2.11a and 4.2.12a). This effect might be related to mountain lee wave breaking and result into a turbulent precipitation pattern with pulses of 30 min intense precipitation. More precipitation events need to be studied to understand this effect around the Haukeliseter site. MEPS does not cover all pulses related to west wind during the course of a day. This is related to the short occurrence of the pulses as well as to the time resolution of the forecast values. Since the prediction values exist only every hour the model might miss some of the intense, 30 min precipitation.

One outcome of the presented study is that MEPS is able to resolve the local topography and predicts the wind direction correctly. The variability between the ensemble members is smaller for precipitation related to south-easterly winds (Figures 4.2.15a to 4.2.15e). It did not cover the south-east wind direction on 21 December 2016 (Figure 4.1.1c), which must be related to the local topography.
For large scale south-westerly flow the model simulates south direction rather than south-easterly flow along the valley. As seen in Figure 4.2.17, the wind should flow along the 7.2° E, since a higher (1500 m to 1650 m) elevation is to the west and a 1350 m high mountain to the east. True prediction of 10 m wind direction (Figure 4.1.1c, **??**, 4.1.2c, **??**, 4.1.3c, and 4.1.4c) leads to the correct estimation of frozen precipitation patterns, such as up-slope (south-easterlies) on 21 (Figure 4.2.8) and 23 December 2016 (4.2.10) and pulsing on 22, 24, 25, and 26 December 2016 (westerlies, Fig-

ure 4.2.8, 4.2.9, and **??**).

Section 4.2.3 describes the overestimation of surface snow accumulation during the intensification of the extreme storm. MEPS forecast in Figure 4.2.5a, b, and c show more ground accumulation than observed for 24 to 26 December 2016. Aim of this thesis is to analyse if the wind might have had an influence on the surface measurement of the double fence, which could not be shown, even if 10 % under-catch by the double fence gauge is assumed (Table 4.2.4). A comparison of the hourly values of MEPS, show neither on 24, 25, and 26 December 2016 high snow amounts in the lower most profiles compared to the estimated SWC (Figure 4.2.11b, 4.2.12b, and b). Figure B.2.1 shows values of very high instantaneous snow water content for individual ensemble members, but no prominent sign of overestimation when the surface simulated too much surface precipitation amount.
During 24 to 26 December 2016 the wind is constantly from the west with higher wind speeds observed than during 21 to 23 December 2016 (**??**). Figure 4.1.6c and d indicate a better correlation for the observed and forecasted wind directions when precipitation overestimation occurred (24 to 26 December 2016). During 24 and 26 December 2016, observed wind speeds were higher, up to 20 $\mathrm{m\,s^{-1}}$, than on the previous days. As Figure 4.1.7a and b present the correlation between observation and forecasts is low for high wind speeds. The high wind speeds from the west followed a pulsing storm pattern with alternating high and low snowfall (e.g. 22 and 24 December 2016, Figure 4.2.9 and 4.2.11). MEPS is able to forecast the pulsing pattern for initialisations longer than 24 h prior. Since the model estimates the wind direction correctly for west wind and local mountain effects it follows that there seems to be an interaction issue between modelled precipitation and the surface accumulation. Hourly ensemble mean of the instantaneous values could have led to a misinterpretation of the here presented results. Furthermore, this study presents only a first look for a comparison between observations up to 3 km of precipitation to MEPS forecast for an extreme event.
The ensemble variability in Figure 4.2.15 shows that the ensemble members are divided between the existence of the exact precipitation pulsing.

While the wind direction of MEPS has a good agreement, at least for west wind, the wind speed shows larger values over all days (Figure 4.1.6c, d, 4.1.7a, b). Although MEPS includes ten perturbed ensemble members, the too high wind speed forecasts in AROME-MetCoOp is not resolved in extreme situations. As Müller et al. [2017] pointed out, higher wind speeds are in general better forecasted in AROME-MetCoOp than in ECMWF. The improved representation of surface parameters in the small-scale model MEPS is important when warnings are send out by the meteorological services for extreme weather events. This is an advantage for fine scale forecast models, especially in Norway, where the topography changes from sea to mountainous terrain on small spatial scale.

The previous chapters have indicated that the regional model MEPS is able to predict larger scale phenomena. This might be related to the outer boundary condition ECMWF or the Christmas 2016 extreme event was more predictable for large scale phenomena. In general, surface parameters such as sea level pressure and temperature were predicted well in MEPS. Only wind speed and precipitation accumulation showed overestimation in MEPS predictions. Wind speed forecasts were higher than observed wind speed. Related to the representation of the orography in MEPS the general overestimation of wind speed could already be apparent in the deterministic version AROME-MetCoOp.

Sensitivity studies for the outer boundary could help to understand how the influence of ECMWF forecast on the MEPS predictions for local meteorological effects. ECMWF as boundary condition might not have reached its background climate state when MEPS was initiated during the event. This could also have contributed to the overestimation of wind speed and surface accumulation. A comparison between ECMWF forecast and MEPS will verify if this might be the case. Re-analysis data can help to show the uncertainty in the initial and boundary conditions. A re-run with analysis data from ECMWF could possibly improve the original forecast. It will be interesting to initiate MEPS with new boundary conditions from ECMWF. Even though meteorological observations are transmitted to ECMWF at the meteorological observation times, not all observations will be communicated in time for the initialisation. An initialisation now with all available observations inside ECMWF will help to see an influence on the overestimation of wind and precipitation accumulation.

Another approach could be to perturb the deterministic forecast in another way. Different perturbations might lead to a better correlation between observation and MEPS forecast at the ground. Furthermore, the choice of using the closest grid point to Haukeliseter might not have been the best approach. Using four nearby grid points instead of only one could help to verify if overestimations of MEPS forecasts would still be present compared to observations.

Even though MEPS performed well in the vertical by relating the wind to the storm structure correctly, it will be interesting to investigate the presented results with a higher time resolution to resolve for the short pulses. Since MEPS overestimates the surface accumulation and the vertical SWC of ensemble means show to be in general smaller than the estimated snow water content, the afore mentioned solution helps to investigate the overestimation of snowfall at the surface and the relationship between the vertical forecast and surface prediction model.

The local effect of pulsing patterns related to westerlies should be examined. To understand if e.g. wave breaking occurs at the mountain to the west or if it is an effect of local surface fronts.

With the forecast output more than 24 h prior can risk notice be send out to the population and rescue teams can prepare in advance. Furthermore, roads and train tracks can be closed to increase the safety.

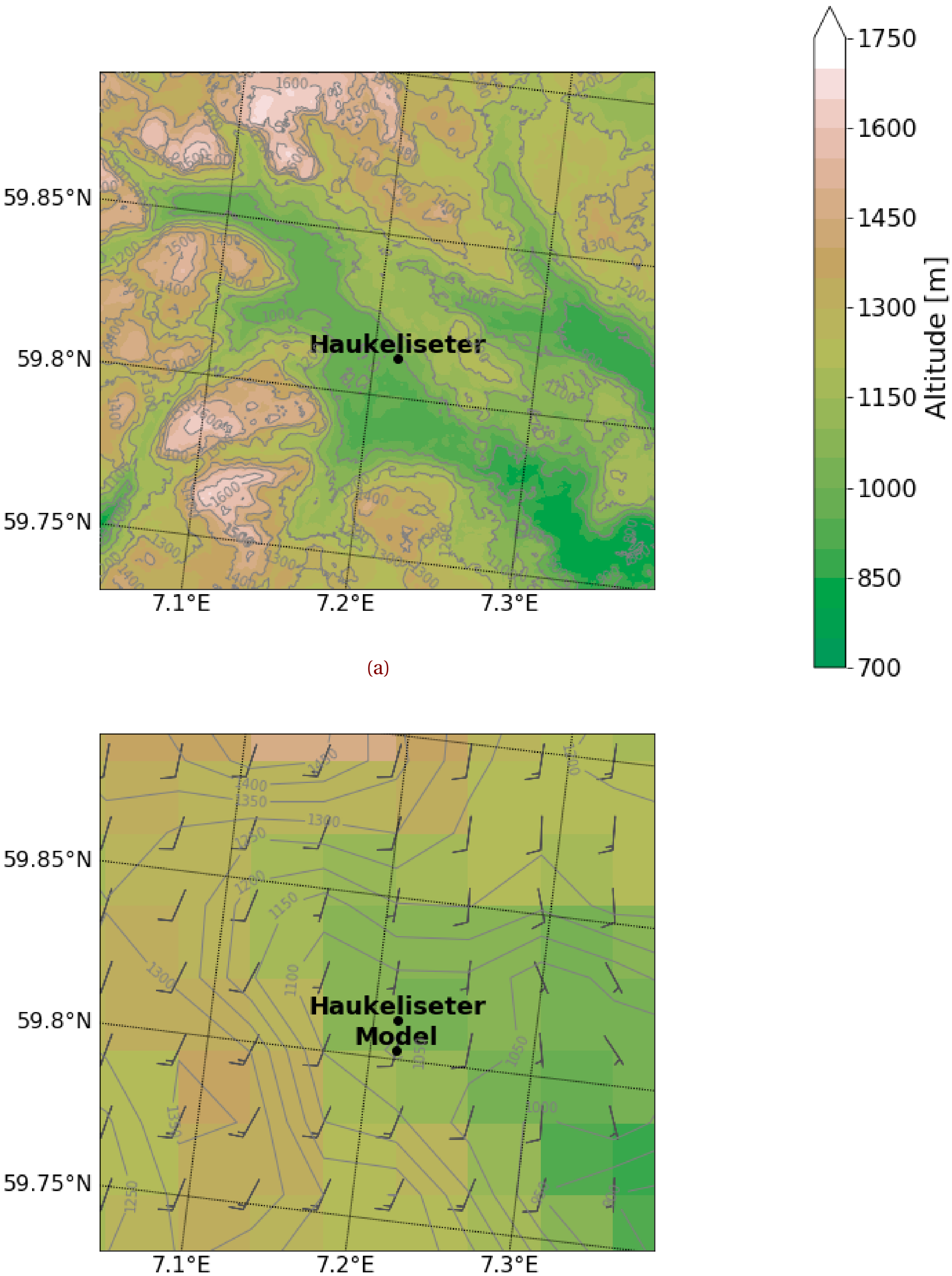

(a)

(b)

Figure 4.2.17: Topography around Haukeliseter. In a the DTM 10 m Terrain Model (UTM33) from Geonorge [2018]. Contours and shading according to the colour bar. b: Representation of the topography and the closest grid point to the measurement site Haukeliseter in MEPS. Contours and shading present the elevation of the grid cells. Wind barbs indicate the wind direction and speed for initialisations on 23 December 2016 at 0 UTC after 18 h lead time

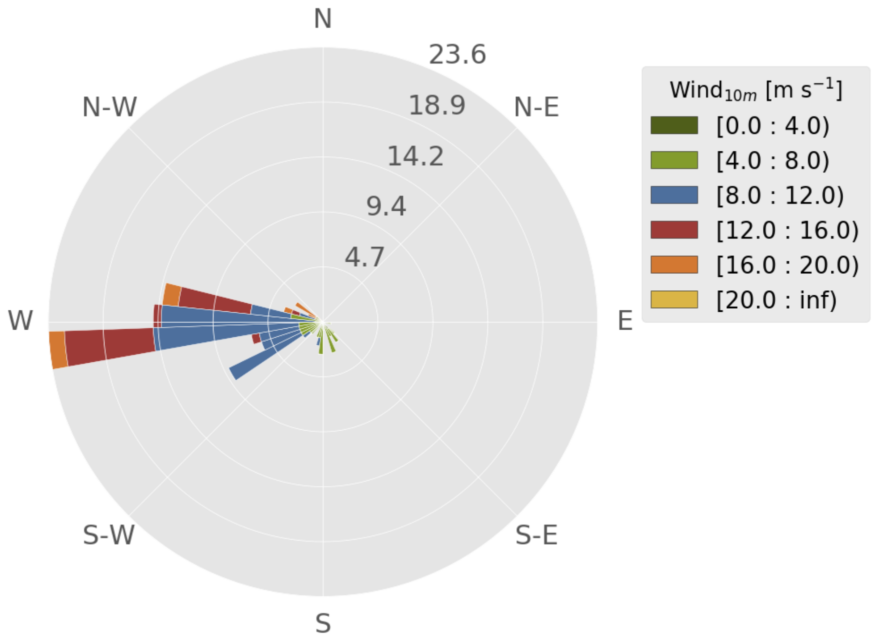

Figure 4.2.18: 10 m wind observed at Haukeliseter during 21 and 26 December 2016. Wind speed according to the colour bar.

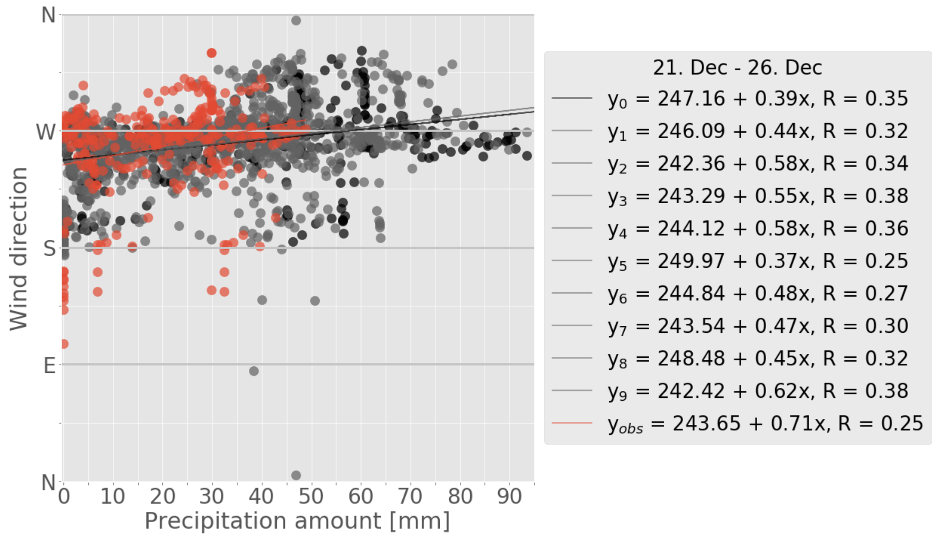

(a)

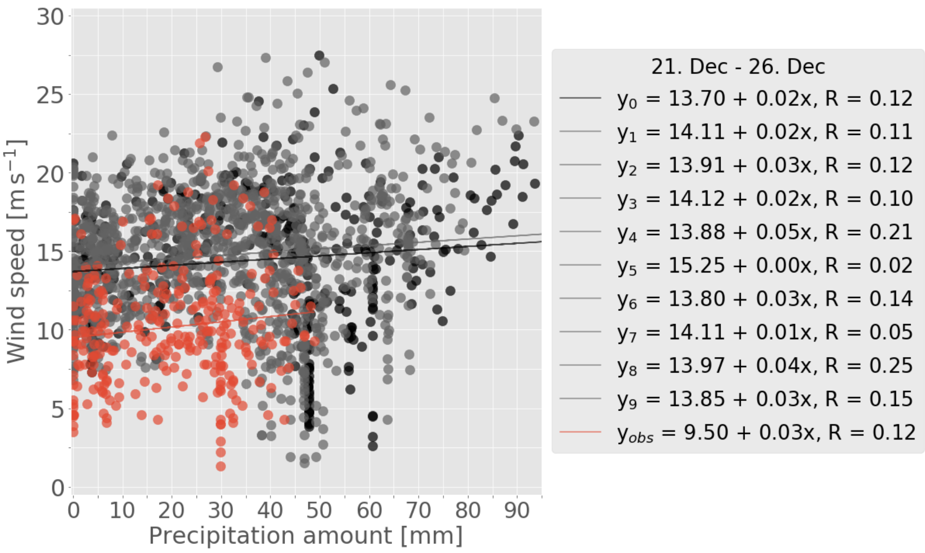

(b)

Figure 4.2.19: Correlation between surface precipitation amount accumulated over 48 h and a: 10 m wind direction, and **??** 10 m wind speed. Red indicating the observations. Black the deterministic MEPS forecast and grey the perturbed ensemble member.

List of Abbreviations

ACC	Accretion
AGG	Aggregation
AR	Atmospheric River
AROME	Applications of Research to Operations at Mesoscale
AUT	Autoconversion
BER	Bergeron-Findeisen process
C3VP	Canadian CloudSat-CALIPSO Validation Project
CFR	Contact Freezing of Raindrops
CPR	Cloud Profiling Radar
CV	Coefficient of Variation
CVM	Conversion-melting
DDA	Discrete Dipole Approximation
DEP	Deposition
DRY	Dry processes
DT	Dynamic Tropopause
ECMWF	European Centre for Medium-Range Weather Forecasts
EPS	Ensemble Prediction System
FMI	Finnish Meteorological Institute
HEN	Heterogeneous Nucleation
HON	Homogeneous Nucleation
IVT	Integrated Vapour Transport
LWC	Liquid Water Content

MASC	Multi-Angular Snowfall Camera
MEPS	MetCoOp Ensemble Prediction System
Meso-NH	Mesoscale Non-Hydrostatic model
Met-Norway	Norwegian Meteorological Institute
MetCoOp	Meteorological Co-operation on Operational NWP
MLT	Melting
MRR	Micro Rain Radar
MSLP	Mean Sea Level Pressure
NSF	National Science Foundation
NWP	Numerical Weather Prediction
PIP	Precipitation Imaging Package
PSD	Particle Size distribution
RIM	Riming
SMHI	Swedish Meteorological and Hydrological Institute
SWC	Snow Water Content
SWP	Snow Water Path
WCB	Warm Conveyor Belt
WET	Wet processes
WMO	World Meteorological Organization

References

Azad, R. and Sorteberg, A. Extreme daily precipitation in coastal western Norway and the link to atmospheric rivers. *Journal of Geophysical Research: Atmospheres*, 122(4):2080–2095, January 2017. ISSN 2169-8996. doi: 10.1002/2016JD025615. URL https://agupubs.onlinelibrary.wiley.com/doi/abs/10.1002/2016JD025615.

Barnett, T. P., Adam, J. C., and Lettenmaier, D. P. Potential impacts of a warming climate on water availability in snow-dominated regions. *Nature*, 438(7066):303–309, November 2005. ISSN 1476-4687. doi: 10.1038/nature04141. URL https://www.nature.com/articles/nature04141.

Buizza, R., Hollingsworth, A., Lalaurette, F., and Ghelli, A. Probabilistic Predictions of Precipitation Using the ECMWF Ensemble Prediction System. *Wea. Forecasting*, 14(2):168–189, April 1999. ISSN 0882-8156. doi: 10.1175/1520-0434(1999)014<0168:PPOPUT>2.0.CO;2. URL https://journals.ametsoc.org/doi/full/10.1175/1520-0434%281999%29014%3C0168%3APPOPUT%3E2.0.CO%3B2.

Caniaux, G., Redelsperger, J.-L., and Lafore, J.-P. A Numerical Study of the Stratiform Region of a Fast-Moving Squall Line. Part I: General Description and Water and Heat Budgets. *J. Atmos. Sci.*, 51(14):2046–2074, July 1994. ISSN 0022-4928. doi: 10.1175/1520-0469(1994)051<2046:ANSOTS>2.0.CO;2. URL https://journals.ametsoc.org/doi/abs/10.1175/1520-0469(1994)051%3C2046:ANSOTS%3E2.0.CO;2.

Christensen, M. W., Behrangi, A., L'ecuyer, T. S., Wood, N. B., Lebsock, M. D., and Stephens, G. L. Arctic Observation and Reanalysis Integrated System: A New Data Product for Validation and Climate Study. *Bull. Amer. Meteor. Soc.*, 97(6):907–916, January 2016. ISSN 0003-0007. doi: 10.1175/BAMS-D-14-00273.1. URL https://journals.ametsoc.org/doi/10.1175/BAMS-D-14-00273.1.

Cooper, S. J., Wood, N. B., and L'Ecuyer, T. S. A variational technique to estimate snowfall rate from coincident radar, snowflake, and fall-speed observations. *Atmos. Meas. Tech.*, 10(7):2557–2571, July 2017. ISSN 1867-8548. doi: 10.5194/amt-10-2557-2017. URL https://www.atmos-meas-tech.net/10/2557/2017/.

Dahlgren, P. A Comparison Of Two Large Scale Blending Methods. page 16, 2013. URL http://metcoop.org/memo/2013/02-2013-METCOOP-MEMO.PDF.

Dando, P. Introducing the octahedral reduced Gaussian grid, June 2016. URL https://software.ecmwf.int/wiki/display/FCST/Gaussian+grids.

Doviak, R. J. and Zrnic, D. S. *Doppler Radar and Weather Observations*. Courier Corporation, 1993. ISBN 978-0-486-45060-5. Google-Books-ID: ispLkPX9n2UC.

eklima. Norwegian Meteorological Institute, 2016. URL http://sharki.oslo.dnmi.no/portal/page?_pageid=73,39035,73_39049&_dad=portal&_schema=PORTAL.

Færaas, A., Rommetveit, A., Duesund, J., and Senel, E. «Urd» har nådd orkan styrke – flytter seg mot Østlandet, December 2016. URL http://www.yr.no/artikkel/_urd_-har-nadd-orkan-styrke-_-flytter-seg-mot-ostlandet-1.13292245.

Farestveit, E. 80.000 mista radioen under ekstremvêret, December 2016. URL https://www.nrk.no/hordaland/80.000-mista-radioen-under-ekstremveret-1.13294980.

Field, C. B., Barros, V. R., Dokken, D. J., Mach, K. J., Mastrandrea, M. D., Bilir, T. E., Chatterjee, M., Ebi, K. L., Estrada, Y. O., Genova, R. C., Girma, B., Kissel, E. S., Levy, A. N., MacCracken, S., Mastrandrea, P. R., and White, L. L. Summary for policymakers. In: Climate Change 2014: Impacts, Adaptation, and Vulnerability. Part A: Global and Sectoral Aspects. Contribution of Working Group II to the Fifth Assessment Report of the Intergovernmental Panel on Climate Change. *Cambridge: Cambridge University Press*, page 34, 2014.

Foote, G. B. and Du Toit, P. S. Terminal Velocity of Raindrops Aloft. *J. Appl. Meteor.*, 8(2):249–253, April 1969. ISSN 0021-8952. doi: 10.1175/1520-0450(1969)008<0249:TVORA>2.0.CO;2. URL https://journals.ametsoc.org/doi/10.1175/1520-0450%281969%29008%3C0249%3ATVORA%3E2.0.CO%3B2.

Garrett, T. J., Fallgatter, C., Shkurko, K., and Howlett, D. Fall speed measurement and high-resolution multi-angle photography of hydrometeors in free fall. *Atmos. Meas. Tech.*, 5(11):2625–2633, November 2012. ISSN 1867-8548. doi: 10.5194/amt-5-2625-2012. URL https://www.atmos-meas-tech.net/5/2625/2012/.

Geonor Inc. T-200b All Weather Precipitation – Rain Gauge, 2015. URL http://geonor.com/live/products/weather-instruments/t-200b-weather-precipitation-rain-gauge/.

Geonorge. DTM 10 Terrengmodell (UTM33) - Kartverket - Kartkatalogen, May 2018. URL https://kartkatalog.geonorge.no/metadata/uuid/dddbb667-1303-4ac5-8640-7ec04c0e3918.

Goodison, B. E., Louie, P. Y. T., and Yang, D. WMO Solid Precipitation Measurement Intercomparison: Final Report. Instruments and Observing Methods Rep. 67, WMO/TD-No. 872,. *World Meteorological Organization, Geneva, Switzerland*, page 318, 1998.

Gowan, T. M., Steenburgh, W. J., and Schwartz, C. S. Validation of Mountain Precipitation Forecasts from the Convection-Permitting NCAR Ensemble and Operational Forecast Systems over the Western United States. *Wea. Forecasting*, 33(3):739–765, June 2018. ISSN 0882-8156, 1520-0434. doi: 10.1175/WAF-D-17-0144.1. URL http://journals.ametsoc.org/doi/10.1175/WAF-D-17-0144.1.

Hansen, B. B., Isaksen, K., Benestad, R. E., Kohler, J., Pedersen, Ø. Ø., Loe, L. E., Coulson, S. J., Larsen, J. O., and Varpe, Ø. Warmer and wetter winters: characteristics and implications of an extreme weather event in the High Arctic. *Environ. Res. Lett.*, 9(11):114021, 2014. ISSN 1748-9326. doi: 10.1088/1748-9326/9/11/114021. URL http://stacks.iop.org/1748-9326/9/i=11/a=114021.

Homleid, M. and Tveter, F. T. Verification of operational weather prediction models september to november 2015. *METInfo Rep*, 16:2016, 2016. URL https://www.met.no/publikasjoner/

met-info/met-info-2016/_/attachment/download/b0463915-cba0-42ac-8539-4233ae2bf01c:3d71565a27f88085373199a33ab8569151c144e9/MET-info-22-2016.pdf.

Hudak, D., Barker, H., Rodriguez, P., and Donovan, D. The Canadian CloudSat Validation Project. *4th ERAD*, September 2006. URL http://www.crahi.upc.edu/ERAD2006/proceedingsMask/00165.pdf. Barcelona, Spain.

Hurrell, J. W. Decadal Trends in the North Atlantic Oscillation: Regional Temperatures and Precipitation. *Science*, 269(5224):676–679, August 1995. ISSN 0036-8075, 1095-9203. doi: 10.1126/science.269.5224.676. URL http://science.sciencemag.org/content/269/5224/676.

Joos, H. and Wernli, H. Influence of microphysical processes on the potential vorticity development in a warm conveyor belt: a case-study with the limited-area model COSMO. *Q. J. Royal Meteorol. Soc.*, 138(663):407–418, January 2012. ISSN 00359009. doi: 10.1002/qj.934. URL http://doi.wiley.com/10.1002/qj.934.

Kalnay, E. *Atmospheric modeling, data assimilation and predictability*. Cambridge University Press, Cambridge, 2003. ISBN 978-0-521-79179-3.

Kartverket. Norgeskart, November 2018. URL http://www.norgeskart.no/?_ga=2.7509489.291164698.1524482471-1352211079.1517515119#!?project=seeiendom&layers=1002,1015&zoom=4&lat=7197864.00&lon=396722.00.

Kochendorfer, J., Nitu, R., Wolff, M., Mekis, E., Rasmussen, R., Baker, B., Earle, M. E., Reverdin, A., Wong, K., Smith, C. D., Yang, D., Roulet, Y.-A., Buisan, S., Laine, T., Lee, G., Aceituno, J. L. C., Alastrué, J., Isaksen, K., Meyers, T., Brækkan, R., Landolt, S., Jachcik, A., and Poikonen, A. Analysis of single-Alter-shielded and unshielded measurements of mixed and solid precipitation from WMO-SPICE. *Hydrol. Earth Syst. Sci.*, 21(7):3525–3542, July 2017. ISSN 1607-7938. doi: 10.5194/hess-21-3525-2017. URL https://www.hydrol-earth-syst-sci.net/21/3525/2017/.

Køltzow, M. A. Ø. Spin-up time of MEPS. Private Communication, 2018.

Kulie, M. S. and Bennartz, R. Utilizing Spaceborne Radars to Retrieve Dry Snowfall. *J. Appl. Meteor. Climatol.*, 48(12):2564–2580, January 2009. ISSN 1558-8424. doi: 10.1175/2009JAMC2193.1. URL http://journals.ametsoc.org/doi/abs/10.1175/2009JAMC2193.1.

Kulie, M. S., Milani, L., Wood, N. B., Tushaus, S. A., Bennartz, R., and L'Ecuyer, T. S. A Shallow Cumuliform Snowfall Census Using Spaceborne Radar. *J. Hydrometeor.*, 17(4):1261–1279, February 2016. ISSN 1525-755X. doi: 10.1175/JHM-D-15-0123.1. URL https://journals.ametsoc.org/doi/abs/10.1175/JHM-D-15-0123.1.

Køltzow, M. A. MetCoOp EPS - A convection permitting ensemble prediction system, October 2017.

L'Ecuyer, T. S. AOS 441 - Satellite and Radar Meteorology. January 2017. URL https://lecuyer.aos.wisc.edu/aos441.

Liu G. Deriving snow cloud characteristics from CloudSat observations. *J. Geophys. Res. Atmos.*, 113 (D8), September 2008. ISSN 0148-0227. doi: 10.1029/2007JD009766. URL https://agupubs.onlinelibrary.wiley.com/doi/abs/10.1029/2007JD009766.

Lorenz, E. N. Atmospheric Predictability as Revealed by Naturally Occurring Analogues. *J. Atmos. Sci.*, 26(4):636–646, July 1969. ISSN 0022-4928. doi: 10.1175/1520-0469(1969)26<636:APARBN>2.0.CO;2. URL https://journals.ametsoc.org/doi/abs/10.1175/1520-0469%281969%2926%3C636%3AAPARBN%3E2.0.CO%3B2.

Markowski, P. and Richardson, Y. *Mesoscale Meteorology in Midlatitudes*. John Wiley & Sons, September 2011. ISBN 978-1-119-96667-8. Google-Books-ID: MDeYosfLLEYC.

Martin, J. E. *Mid-Latitude Atmospheric Dynamics: A First Course*. Wiley, May 2006. ISBN 978-0-470-86466-1.

McCumber, M., Tao, W.-K., Simpson, J., Penc, R., and Soong, S.-T. Comparison of Ice-Phase Microphysical Parameterization Schemes Using Numerical Simulations of Tropical Convection. *J. Appl. Meteor.*, 30(7):985–1004, July 1991. ISSN 0894-8763. doi: 10.1175/1520-0450-30.7.985. URL https://journals.ametsoc.org/doi/abs/10.1175/1520-0450-30.7.985.

Meehl, G. A., Karl, T., Easterling, D. R., Changnon, S., Pielke, R., Changnon, D., Evans, J., Groisman, P. Y., Knutson, T. R., Kunkel, K. E., Mearns, L. O., Parmesan, C., Pulwarty, R., Root, T., Sylves, R. T., Whetton, P., and Zwiers, F. An Introduction to Trends in Extreme Weather and Climate Events: Observations, Socioeconomic Impacts, Terrestrial Ecological Impacts, and Model Projections. *Bull. Amer. Meteor. Soc.*, 81(3):413–416, March 2000. ISSN 0003-0007. doi: 10.1175/1520-0477(2000)081<0413:AITTIE>2.3.CO;2. URL https://journals.ametsoc.org/doi/abs/10.1175/1520-0477(2000)081%3C0413:AITTIE%3E2.3.CO;2.

MetCoOp Wiki. Description of MEPS, December 2017. URL https://metcoop.smhi.se/dokuwiki/nwp/metcoop/.

METEK, M. M. G. Micro Rain Radar MRR-2, October 2010. URL http://metek.de/wp-content/uploads/2014/05/Metek-Micro-Rain-Radar-MRR-2-Datasheet.pdf.

Meteo France. The Meso-NH Atmospheric Simulation System: Scientific Documentation, Part III: Physics, January 2009.

Meteorologene. "Her kommer #Urd! Selve Lavtrykksenteret treffer Møre og Romsdal, men den sterkeste vinden kommer sør for Stad. #SørNorge" 26 December 2016, 9:34am, 2016. URL https://twitter.com/Meteorologene.

Moore, R. Large-scale dynamics inducing atmospheric rivers and extreme precipitation over norway. unpublished.

Müller, M., Homleid, M., Ivarsson, K.-I., Køltzow, M. A. Ø., Lindskog, M., Midtbø, K. H., Andrae, U., Aspelien, T., Berggren, L., Bjørge, D., Dahlgren, P., Kristiansen, J., Randriamampianina, R., Ridal, M., and Vignes, O. AROME-MetCoOp: A Nordic Convective-Scale Operational Weather Prediction Model. *Wea. Forecasting*, 32(2):609–627, January 2017. ISSN 0882-8156. doi: 10.1175/WAF-D-16-0099.1. URL http://journals.ametsoc.org/doi/abs/10.1175/WAF-D-16-0099.1.

Newman, A. J., Kucera, P. A., and Bliven, L. F. Presenting the Snowflake Video Imager (SVI). *J. Atmos. Oceanic Technol.*, 26(2):167–179, February 2009. ISSN 0739-0572. doi: 10.1175/2008JTECHA1148.1. URL https://journals.ametsoc.org/doi/abs/10.1175/2008JTECHA1148.1.

Nielsen-Gammon, J. W. A Visualization of the Global Dynamic Tropopause. *Bull.*

Amer. Meteor. Soc., 82(6):1151–1168, June 2001. ISSN 0003-0007. doi: 10.1175/1520-0477(2001)082<1151:AVOTGD>2.3.CO;2. URL https://journals.ametsoc.org/doi/abs/10.1175/1520-0477(2001)082%3C1151:AVOTGD%3E2.3.CO;2.

Noh, Y.-J., Liu, G., Seo, E.-K., Wang, J. R., and Aonashi, K. Development of a snowfall retrieval algorithm at high microwave frequencies. *J. Geophys. Res*, 111(D22), November 2006. ISSN 2156-2202. doi: 10.1029/2005JD006826. URL https://agupubs.onlinelibrary.wiley.com/doi/abs/10.1029/2005JD006826.

Norin, L., Devasthale, A., L'Ecuyer, T. S., Wood, N. B., and Smalley, M. Intercomparison of snowfall estimates derived from the CloudSat Cloud Profiling Radar and the ground-based weather radar network over Sweden. *Atmos. Meas. Tech.*, 8(12):5009–5021, December 2015. ISSN 1867-8548. doi: 10.5194/amt-8-5009-2015. URL https://www.atmos-meas-tech.net/8/5009/2015/.

Norwegian Meteorological Institute. MET Norway Thredds Service, 2016. URL http://thredds.met.no/thredds/catalog/meps25epsarchive/catalog.html.

Olsen, A.-M. and Granerød, M. Ekstremværrapport. Hendelse: Urd 26. desember met. info. no. 18/2017 ISSN X METEOROLOGI Bergen, - PDF, September 2017. URL http://docplayer.me/48734203-Ekstremvaerrapport-hendelse-urd-26-desember-met-info-no-18-2017-issn-x-meteorologi-bergen.html.

Palerme, C., Kay, J. E., Genthon, C., L'Ecuyer, T., Wood, N. B., and Claud, C. How much snow falls on the Antarctic ice sheet? *The Cryosphere*, 8(4):1577–1587, August 2014. ISSN 1994-0424. doi: 10.5194/tc-8-1577-2014. URL https://www.the-cryosphere.net/8/1577/2014/.

Palerme, C., Genthon, C., Claud, C., Kay, J. E., Wood, N. B., and L'Ecuyer, T. Evaluation of current and projected Antarctic precipitation in CMIP5 models. *Clim. Dyn.*, 48(1-2):225–239, January 2017. ISSN 0930-7575, 1432-0894. doi: 10.1007/s00382-016-3071-1. URL https://link.springer.com/article/10.1007/s00382-016-3071-1.

Pedersen, K. and Rommetveit, A. Hva er et «ekstremvær»?, November 2013. URL http://www.yr.no/artikkel/hva-er-et-_ekstremvaer__-1.7890946.

Peel, M. C., Finlayson, B. L., and Mcmahon, T. A. Updated world map of the Köppen-Geiger climate classification. *Hydrology and Earth System Sciences Discussions*, 4(2):439–473, March 2007. URL https://hal.archives-ouvertes.fr/hal-00298818.

Petroliagis, T., Buizza, R., Lanzinger, A., and Palmer, T. N. Potential use of the ECMWF Ensemble Prediction System in cases of extreme weather events. *Meteorological Applications*, 4(1):69–84, March 1997. ISSN 1469-8080, 1350-4827. URL https://www.cambridge.org/core/journals/meteorological-applications/article/potential-use-of-the-ecmwf-ensemble-prediction-system-in-cases-of-extreme-weather-events/C63050704CB35CD43BC4E5998A390DDC.

Pinty, J.-P. and Jabouille, P. A mixed-phased cloud parameterization for use in a mesoscale non-hydrostatic model: Simulations of a squall line and of orographic precipitation. pages 217–220. Amer. Meteor. Soc., 1998.

Rinehart, R. E. *Radar for Meteorologists: Or You, Too, Can be a Radar Meteorologist.* Rinehart Publications, 2010. ISBN 978-0-9658002-3-5. Google-Books-ID: VqatcQAACAAJ.

Rutz, J. J., Steenburgh, W. J., and Ralph, F. M. Climatological Characteristics of Atmospheric Rivers and Their Inland Penetration over the Western United States. *Mon. Wea. Rev.*, 142(2):905–921, January 2014. ISSN 0027-0644. doi: 10.1175/MWR-D-13-00168.1. URL http://journals.ametsoc.org/doi/abs/10.1175/MWR-D-13-00168.1.

Ruud, S., Carr Ekroll, H., Bakke Foss, A., Torgersen, H. O., and Annar Holm, P. To tonn tungt skilt blåste ned da ekstremværet traff Oslo og Østlandet i natt, December 2016. URL https://www.aftenposten.no/article/ap-2z6wy.html.

Schirle, C. Characterization of snowfall at high latitudes using an optimal estimation-based retrieval algorithm. Private Communication, 2018.

Shi, W., L'Heureux, M., and Halpert, M. Climate Diagnostics Bulletin - December 2016, Near Real-Time Ocean/Atmosphere: Monitoring, Assessments, and Prediction. Technical report, Climate Prediction Center, 2016. URL http://origin.cpc.ncep.noaa.gov/products/CDB/CDB_Archive_pdf/PDF/CDB.dec2016_color.pdf.

Skofronick-Jackson, G. M., Kim, M.-J., Weinman, J. A., and Chang, D.-E. A physical model to determine snowfall over land by microwave radiometry. *IEEE Geosci. Remote Sens. Lett.*, 42(5): 1047–1058, May 2004. ISSN 0196-2892. doi: 10.1109/TGRS.2004.825585.

Stephens, G. L. *Remote Sensing of the Lower Atmosphere: An Introduction.* Oxford University Press, 1994. ISBN 978-0-19-508188-6. Google-Books-ID: 2FcRAQAAIAAJ.

Stocker, T. F., Qin, D., Plattner, G.-K., Tignor, M. M. B., Allen, S. K., Boschung, J., Nauels, A., Xia, Y., Bex, V., and Midgley, P. M. Working Group I Contribution to the Fifth Assessment Report of the Intergovernmental Panel on Climate Change. *Cambridge: Cambridge University Press*, page 14, 2013.

Sun, J. Convective-scale assimilation of radar data: progress and challenges. *Quarterly Journal of the Royal Meteorological Society*, 131(613):3439–3463, 2005. ISSN 1477-870X. doi: 10.1256/qj.05.149. URL https://rmets.onlinelibrary.wiley.com/doi/abs/10.1256/qj.05.149.

Uvo, C. B. Analysis and regionalization of northern European winter precipitation based on its relationship with the North Atlantic oscillation. *International Journal of Climatology*, 23(10):1185–1194, July 2003. ISSN 1097-0088. doi: 10.1002/joc.930. URL https://rmets.onlinelibrary.wiley.com/doi/abs/10.1002/joc.930.

Warner, T. T., Peterson, R. A., and Treadon, R. E. A Tutorial on Lateral Boundary Conditions as a Basic and Potentially Serious Limitation to Regional Numerical Weather Prediction. *Bull. Amer. Meteor. Soc.*, 78(11):2599–2618, November 1997. ISSN 0003-0007. doi: 10.1175/1520-0477(1997)078<2599:ATOLBC>2.0.CO;2. URL https://journals.ametsoc.org/doi/abs/10.1175/1520-0477(1997)078%3C2599:ATOLBC%3E2.0.CO%3B2.

Wolff, M. A. WMO Solid Precipitation Intercomparison Experiment (WMO-SPICE), Ch. 4.2.4 Precipitation measurements in areas with high winds and/or complex terrain. unpublished.

Wolff, M. A., Brækkan, R., Isaksen, K., and Ruud, E. A new testsite for wind correction of precipitation measurements at a mountain plateau in southern Norway. In *Proceedings of WMO Technical Conference on Meteorological and Environmental Instruments and Methods of Observation (TECO–2010). Instruments and Observing Methods Report*, 2010.

Wolff, M. A., Isaksen, K., Brækkan, R., Alfnes, E., Petersen-Øverleir, A., and Ruud, E. Measurements of wind-induced loss of solid precipitation: description of a Norwegian field study. *Hydrol. Res.*, 44(1):35–43, February 2013. ISSN 0029-1277, 2224-7955. doi: 10.2166/nh.2012.166. URL http://hr.iwaponline.com/content/44/1/35.

Wolff, M. A., Isaksen, K., Petersen-Øverleir, A., Ødemark, K., Reitan, T., and Brækkan, R. Derivation of a new continuous adjustment function for correcting wind-induced loss of solid precipitation: results of a Norwegian field study. *Hydrol. Earth Syst. Sci.*, 19(2):951–967, February 2015. ISSN 1607-7938. doi: 10.5194/hess-19-951-2015. URL https://www.hydrol-earth-syst-sci.net/19/951/2015/.

Wood, N. B. *Estimation of snow microphysical properties with application to millimeter-wavelength radar retrievals for snowfall rate.* Ph.D., Colorado State University, 2011. URL https://dspace.library.colostate.edu/bitstream/handle/10217/48170/Wood_colostate_0053A_10476.pdf?sequence=1&isAllowed=y.

Wood, N. B., L'Ecuyer, T. S., Vane, D. G., Stephens, G. L., and Partain, P. Level 2c snow profile process description and interface control document. Technical Report, 2013. URL http://www.cloudsat.cira.colostate.edu/sites/default/files/products/files/2C-SNOW-PROFILE_PDICD.P_R04.20130210.pdf.

Wood, N. B., L'Ecuyer, T. S., Heymsfield, A. J., and Stephens, G. L. Microphysical Constraints on Millimeter-Wavelength Scattering Properties of Snow Particles. *J. Appl. Meteor. Climatol.*, 54(4):909–931, January 2015. ISSN 1558-8424. doi: 10.1175/JAMC-D-14-0137.1. URL http://journals.ametsoc.org/doi/10.1175/JAMC-D-14-0137.1.